Testing the performance of tropical cyclone genesis indices in future climates using the HIRAM model

SUZANA J. CAMARGO *

Lamont-Doherty Earth Observatory, Columbia University, Palisades, NY

MICHAEL K. TIPPETT

Department of Applied Physics and Applied Mathematics, Columbia University, New York, NY

Center of Excellence for Climate Change Research, King Abdulaziz University, Jeddah, Saudi Arabia

ADAM H. SOBEL

Department of Earth and Environmental Sciences,

Department of Applied Physics and Applied Mathematics, Columbia University, New York, NY

GABRIEL A. VECCHI, AND MING ZHAO

Geophysics Fluid Dynamics Laboratory - NOAA, Princeton, NJ

**Corresponding author address:* Suzana J. Camargo, Lamont-Doherty Earth Observatory, Columbia University, PO Box 1000, Palisades, NY 10960.

E-mail: suzana@ldeo.columbia.edu

ABSTRACT

Tropical cyclone genesis indices (TCGIs) are functions of the large-scale environment which are designed to be proxies for the probability of tropical cyclone (TC) genesis. While the performance of TCGIs in the current climate can be assessed by comparison to observations of TC formation, their ability to represent future TC activity based on projections of the large-scale environment cannot. Here we examine the performance of TCGIs in high-resolution climate model simulations of current and projected climates, with a particular interest in determining whether the index, when derived from the climatological seasonal cycle and spatial distribution of both TC genesis frequency and large-scale fields from present climate, but then computed from large-scale fields taken from simulations forced with SST patterns derived from coupled simulations of future, warmer, climate scenarios can capture the global mean decreases in TC frequency found in those future scenarios. This decrease is captured only when the humidity predictor is column saturation deficit (the difference between actual and saturation water vapor) rather than relative humidity (the ratio of these quantities). Using saturation deficit with relative SST as the other thermodynamic predictor over-predicts the TC frequency decrease, but using potential intensity as the thermodynamic predictor gives a good prediction of the decrease's magnitude. These positive results appear to depend on the spatial and seasonal patterns in the imposed SST changes; none of the indices captures correctly the frequency decrease in simulations in which the only climate forcings are spatially uniform, whether a globally uniform increase in SST of 2K, or a doubling of CO_2 with no change in SST.

1. Introduction

It is critically important to understand how greenhouse gas-induced climate change will influence tropical cyclone activity. To do this, we have to first know how the large-scale climate will change, and then how the large-scale climate changes will influence tropical cyclones. We focus here on the second question.

Most model projections for the 21st century climate are computed with relatively low-resolution models. Most of the model simulations in the Coupled Model Intercomparison Project (CMIP5), for example, have horizontal grid spacings of order 100 km or greater. While these low-resolution models are able to simulate tropical-cyclone like structures that have grossly similar properties to observed TCs (Bengtsson et al. 1982; Vitart et al. 1997; Camargo et al. 2005, 2007b), these low-resolution model cyclones are inadequate for detailed studies of the relation of TCs to climate. The cyclones are too large and too weak, and in most cases their climatolological distributions in space and time of year are significantly biased (Walsh et al. 2013; Camargo 2013). An emerging generation of high-resolution coupled climate models is enabling the exploration of the climate response of TCs more directly (e.g., Roberts et al. (2009); Delworth et al. (2012); Bell et al. (2013); Kim et al. (2013)), yet these high-resolution models represent a small fraction of the climate models presently used around the globe.

Many methods for examining future tropical cyclone activity involve downscaling the results of global climate models, using the models to predict changes in the large-scale atmospheric and oceanic environmental fields that are statistically associated with tropical cyclone activity, and inferring the likely changes in tropical cyclone statistics from those environmental fields, using alternative ”downscaling” methods, rather than direct simulation by the climate model. Since low-resolution climate models have better skill in simulating the environmental fields than in simulating TC-like structures themselves (e.g., Camargo 2013), these strategies make better use of the climate models. One possibility is to use the large-scale fields of the global models to force regional climate models (Landman et al. 2005; Camargo et al. 2007a; Knutson et al. 2008). Another possibiility is to use a hybrid dynamical-statistical model which generates synthetic storms based on environmental fields output from the models (Emanuel et al. 2006; Emanuel 2006; Vecchi et al. 2011). Still another option for downscaling is to use statistical models for basin-integrated activity (Villarini and Vecchi 2012, 2013).

Another possibility, and the one explored here, is to relate the models' projections to tropical cyclone changes using local (rather than basin-integrated) relationships between the environmental fields and TC activity in the recent historical climate. A local relationship between environmental factors and tropical cyclogenesis, in particular, when expressed as a single number which is a function of environmental variables and proportional to the probability of genesis, is known as a genesis index.

Gray (1979) developed the first genesis index. Gray's index is not appropriate to explore TC activity in the future, as it uses a fixed threshold for sea surface temperature (SST). To the extent that such a threshold is a good predictor, we expect that it will increase as the climate warms (e.g., Johnson and Xie 2010) since relative SST (the difference between local SST and the tropical mean, or another reference such as the tropical mean upper tropospheric temperature) is a better predictor than absolute SST (Vecchi and Soden 2007; Swanson 2008; Ramsay and Sobel 2011). Since then, many other indices have been developed. Most of these improve on Gray's original index by replacing the fixed SST threshold with thermodynamic predictors more appropriate for handling climate change.

One of the most widely used, the genesis potential index (GPI) was developed by Emanuel and Nolan (2004). It replaces SST entirely, using potential intensity instead. The GPI has been used in applications on various time scales, from intraseasonal to climate change Camargo et al. (2007a, 2009); Vecchi and Soden (2007); Nolan et al. (2007); Lyon and Camargo (2009); Yokoi et al. (2009); Yokoi and Takayabu (2009). More recently, Emanuel (2010) modified his original index, using a variable associated with the saturation deficit in place of the relative humidity parameter used in the original index. While having a similar spatial and temporal distribution in the present climate, the saturation deficit differs from relative humidity — being the difference between the specific humidity and its saturation value, rather than the ratio, and thus increasing systematically with warming if relative humidity remains constant — in a way that is consequential, and apparently better, for capturing climate change. Many other alternative indices have been developed, using different predictors or different functional dependences in their indices (DeMaria et al. 2001; Royer et al. 1998; Sall et al. 2006; Bye and Keay 2008; Kotal et al. 2009; Murakami and Wang 2010; Bruyère et al. 2012). A recent intercomparsion of various genesis indices, including the Tippett et al. (2011) index used here, is given in Menkes et al. (2012).

Our goal here is to evaluate how well tropical cyclone indices developed in the present climate are able to predict changes tropical cyclone frequency in future climates. Because these indices are partly empirical; the predictors are selected based on our current physical understanding of the factors that control genesis, but that understanding is imperfect, and the relationships between the predictors and the index are found using only statistics from the historical climate. Thus, it is possible that they will fail to capture the influence of future climate changes on TCs. We cannot perform empirical tests of the indices' ability to capture these changes, since there are no ”observations” of future tropical cyclone activity. As an alternative, we use a perfect model framework to test our index methodology.

Specifically, we use the GFDL high-resolution global climate model HIRAM, forced with specified SST at 50km resolution. This model has been extensively examined in the present and future climates. It has been shown to simulate both the current climatological global distribution of tropical cyclone activity, and recent historical interannual variations in Atlantic tropical cyclone activity, extremely well. It predicts a decrease in global tropical cyclone frequency in a warmer climate, similar to other comparable models (Knutson et al. 2010).

Our procedure is:

i. Use the model's own TCs and large-scale environmental fields, taken from a control simulation, to derive a tropical cyclone genesis index;

ii. compute the resulting index from model environmental fields taken from a simulation of a warmer climate;

iii. compare the future changes in the indices to future changes in the model's own tropical cyclone frequency.

We use the technique developed by Tippett et al. (2011) to generate and test a number of different tropical cyclone genesis indices in this fashion. The indices differ in the predictors that are used. While our interest here is in the changes due to warming, our procedure also ensures that the indices capture the climatological spatial distribution and seasonal cycle of tropical cyclogenesis in the control simulation from which the index is derived. This is an important difference between our method and those involving statistical models which are designed only to capture temporal variations in basin-integrated activity for a single basin. Each method has its advantages; the advantage of the index methodology is that, being based on local relationships between the probability of genesis and the environment, it is closer to a physical theory for genesis (though still not quite being one, since it is partly empirical). An index which captures the seasonal cycle, global spatial distribution, and temporal changes in genesis frequency everywhere — if one were to exist — would have more explanatory power than one which captures only temporal changes in the basin-integrated frequency for a single basin. If the goal is only to predict variations in basin-integrated activity for one basin, a model designed solely for that purpose may be best. Our approach, instead, tests our understanding of the local physics of genesis, to the extent that the indices represent that.

In Section 2, we summarize the procedure used to obtain TCGI in Tippett et al. (2011). In Section 3, we describe the datasets, the HIRAM model, and the model simulations. A summary of the TC activity in the HIRAM model is given in Section 4. We apply the TCGI to HIRAM model in Section 5. Various alternative indices obtained using the HIRAM environmental fields and TCs are tested in Section 6. In section 7, we discuss our results.

2. Developing TCGI

a. Overview of the methodology

One objective of Tippett et al. (2011) was to develop a TCGI using a robust, objective and easily reproducible procedure. Such a procedure allows the index to be re-derived easily when new data sets become available for either the environmental fields or tropical cyclones, or if new hypotheses about which environmental fields should be used as predictors are developed. The statistical method used is Poisson regression. The TCGI in Tippett et al. (2011) was constructed using the observed climatology of tropical cyclogenesis and large-scale variables from the ERA-40 and NCEP/NCAR reanalyses, as well as retrievals of column water vapor from satellite passive microwave observations.

The regression methodology is objective and provides a framework for the selection of the climate variables to be used in the index. This method led us to select four environmental variables for the index, similar but not identical to those used by Emanuel and Nolan (2004): low-level absolute vorticity, relative humidity, relative SST (difference between the SST and mean tropical SST), and vertical wind shear. One result of Tippett et al. (2011) is that the sensitivity of genesis on low-level absolute vorticity saturates after the vorticity exceeds a threshold; using a ”clipped vorticity” parameter to account for this saturation leads to a better fit of the index to the genesis observations. Although the index was fit only to the climatological data, it reproduces some aspects of the interannual variability reasonably well. The same procedure, with different predictors and predictands, was recently applied successfully to describe the relationship of tornado activity over the United States to environmental variables (Tippett et al. 2012).

The fact that the index can be easily re-derived allows us to customize it to the HIRAM model (or any other). It is possible that the model’s relationship between its large-scale climate fields and its simulated TCs is different from the relationships between the same climate fields and TCs in the real climate. Since any index is at least partly empirical, it is possible that an index derived from TC observations and reanalysis fields will not perform well when used with TCs and environmental variables from a model, since the physical relationships between environment ant TCs in the model may be different. To address this problem, we can simply re-derive our index using both TCs and large-scale fields from the model itself. In this case, we know that the resulting index will be faithful to the model's own relationship between environment and TCs, at least in the simulation from which it was derived. If the resulting index, when computed from the warmer climate simulation, successfully predicts changes in the TC genesis statistics, it increases our confidence in both the index methodology and our ability to understand the reasons for the TC changes in the simulated warmer climate.

b. Specifics

For each grid cell (on a latitude-longitude grid chosen to match the environmental data) and calendar month, we fit the index to the total number of TCG events during a 40-year period. We use a log-linear model, such that the logarithm of the expected number of TCs is linearly related to the index derived from the climate variables. We include a term that takes into account the convergence of the meridians, so that our index has dimensions of the number of TCG events per unit surface area. We use the maximized log-likelihood and the Akaike information criteria (Kaike 1973) to measure the model fit, and attempt to avoid the selection of useless predictors and over-fitting. We use a quasi-Poisson method in which the coefficient estimates are the same as in Poisson regression, but their standard errors are inflated to reflect over-dispersion. A characteristic of the Poisson regression model is that the coefficients of the regression can be interpreted as sensitivities.

The form of the Poisson regression model is, for example:

$$\mu = \exp(b + b_\eta \eta + b_H H + b_T T + b_V V + \log \cos \phi),$$

where μ is the expected number of tropical cyclone genesis events per month in a 40-year climatological period, b is a constant term, and ϕ is latitude. Here η, H, T and V are, respectively, the absolute vorticity at 850hPa in 10^5, the column relative humidity in percent, relative SST in °C and vertical wind shear between 850hPa and 200hPa levels in m/s. The best fit obtained in Tippett et al. (2011), using reanalysis fields to compute these predictors, together with observed TC climatology data, has the following coefficients: $b = -11.96$, $b_\eta = 1.12$, $b_H = 0.12$, $b_T = 0.46$ and $b_V = -0.13$. Here, we will consider these same predictors, but also will consider possible substitutes for H and T.

We first apply the TCGI obtained from reanalysis to the HIRAM model fields and compare it with the number of TCs in the HIRAM model. In the second part of the analysis, we will derive the index from the HIRAM model fields and its TCs in the present climate, performing the Poisson regression on those quantities to obtain a new TCGI from the HIRAM model itself (TCGI-H). Having derived this index from the HIRAM control simulation run over historical SST, we then compute the index using fields from HIRAM simulations with warmer SST, and assess whether the index captures the TC frequency changes simulated directly by the model. We repeat this procedure using multiple different choices for the predictors. We then derive indices using environmental fields and TCs taken directly from the warmer, future climate simulations in HIRAM, in order to examine the changes in the index that result.

3. Data and HIRAM models and simulations

The observed tropical cyclone data are from the best-track datasets of the National Hurricane Center for the North Atlantic and eastern North Pacific (NHC 2013) and the Joint Typhoon Warning Center for the North Indian, western North Pacific and southern Hemisphere (JTWC 2013). The reanalysis fields used to calculate the TCGI are from the NCEP-NCAR reanalysis (Kalnay et al. 1996; Kistler et al. 2001) and the ERA-40 reanalysis (Uppala et al. 2005).

The HIRAM model is a modified version of the GFDL AM2.1 model, as described in detail in Zhao et al. (2009). The version used here has 50 km horizontal grid spacing. The tropical cyclone activity in this model has been examined in many studies, including Zhao et al. (2009), Zhao et al. (2010), Zhao and Held (2010) and Zhao and Held (2012). The climatological TC activity in the HIRAM model is similar to that in the observations in its spatial and temporal characteristics, although the storm frequency is biased slightly low in the North Atlantic, eastern North Pacific, South Indian basins, and slightly high in the western North Pacific and South Pacific. The HIRAM model is able to reproduce the interannual variability and trends of the TC activity in the period 1981-2005 in the North Atlantic with a high degree of fidelity when forced with observed SST. The model is skillful in interannual hindcast mode (i.e., given the SST) in most basins, with exception of the North Indian Ocean.

We will examine the set of simulations with the HIRAM model forced by different specified SST fields. The same simulations were discussed in Zhao et al. (2009) and Zhao and Held (2012).Each SST field is a function of position and time of year, but has no interannual or sub-monthly variability. The first simulation is a 25-year control run, in which the model is forced with the climatological SST from the Hadley Center. For the future climate runs, the climatological SSTs are modified by the addition of SST anomalies from the CMIP3 simulations (Zhao and Held 2012). The atmospheric CO_2 concentration is also increased in the model to be consistent with the A1B scenario for the period 2081-2100, from which the SST anomalies were calculated. The anomalies were calculated as the differences between the multi-model ensemble mean 2081-2100 SSTs in the A1B scenario with the the SSTs in the historical simulations in the period 2001-2020 for the multi-model ensemble mean. The simulation forced with the SSTs anomalies from the multi-model ensemble mean is called ”warm” here and lasts 20 years. The SST anomalies are calculated separately for each month and grid point and are discussed in Zhao and Held (2012).

The two final simulations last 25 years each. In the first one, the SST is kept at the present climatological values and only the CO_2 in the model is doubled ($2xCO_2$). In the second one, a uniform warming of 2K is added to the climatological SST, but CO_2 is not increased; this is called the ”plus 2K” or ”p2K” simulation. The response of the HIRAM model to an increase of CO_2, with fixed SST, and comparison of that to the response in the p2K simulation, was analyzed by Held and Zhao (2011). Table 1 summarizes the 12 simulations considered in this study.

4. Tropical cyclone Activity in the HIRAM model

The tropical cyclone activity in the HIRAM has been discussed extensively in previous studies Zhao et al. (2009, 2010); Zhao and Held (2010, 2012); Held and Zhao (2011). Here we give only a short summary of the results. The algorithm used to define and track model storms is based on Vitart et al. (1997, 2003); Knutson et al. (2007) and described in detail in the appendix B of Zhao et al. (2009).

The first position density and the tracks in both observations and the control simulation with the HIRAM model are shown in Fig. 1. The model's first position density pattern is quite similar to the observed pattern. Biases are noticeable only in a few regions. For example, storms form in the model, unrealistically, near the Nordeste coast of Brazil. The genesis density in the central North Pacific is too high. The genesis rate of subtropical storms is greater than that in observations in the southern hemisphere.

The HIRAM tracks are also, overall, very similar to observed tracks. In some regions the HIRAM tracks tend to be longer than the observed ones, especially in the southern hemisphere, the eastern North Pacific and Arabian Sea.

The mean numbers of storms per month in both hemispheres and in a few individual basins in the HIRAM control run and in observations are shown in Fig. 2. The seasonal cycle of HIRAM NTC is very similar to the observations in both hemipheres. However, in both hemispheres, the model produces too many TCs in the off season. In the peak season of each hemisphere, the model NTCs is very close to the observations, but is slightly below the observed mean in August (northern hemisphere) and February (southern hemisphere). When we examine a few individual basins, there are regions in which the model performs better than in others. Some biases are noticeable. For instance, while the model has a tendency to produce too many TCs in the South Indian Ocean (Fig. 2(c)), the peak season in the Australian region (Fig. 2(d)) has too few TCs. The formation of storms in the off season is more concentrated in the western North Pacific (Fig. 2(e)) than in the North Atlantic (Fig. 2(f)).

In summary, as shown in many previous papers, the HIRAM model's TC activity in the present climate is very realistic with respect to the seasonal cycle, location, and shapes of the tracks. This suggests that the model ought to be a good tool with which to examine frequency changes of TCs in various future scenarios.

Our main interest in this analysis is to determine to what extent the genesis indices are able to predict the differences between the future and present TC frequency. Knutson et al. (2010) has showed that high-resolution models agree on two main robust results regarding future TC activity: a slight reduction in the global frequency of TCs, and the a shift towards more intense storms. The magnitudes of these changes vary from one model to the next. The global reduction in frequency is a good test for a genesis index derived by fitting the spatial and seasonal variations in genesis. However, in contrast with these results, a recent downscaling of the CMIP5 models led to an increase in the global TC frequency in the future (Emanuel 2013).

Fig. 3 shows the global number of TCs in the present and future cases forced with SST anomalies, while the differences in first position climatology between future cases and the present are shown in Fig. 4. In all future simulations, there is a reduction of the number of TCs in the future (with different magnitudes), depending on the SST pattern. This is the main issue we want to address here: how well can the TCGI (and other genesis indices) reproduce the global reduction of TCs in the future runs, while still capturing the spatial and seasonal structure of genesis in the control climate? We will use the HIRAM model's own TCs and environmental variables to examine this question in the next sections.

5. TCGI-R applied to HIRAM

As a first step in our analysis, we applied the TCGI developed using Reanalysis fields (TCGI-R Tippett et al. 2011) to data from the HIRAM model. We calculated the values of the TCGI-R using the monthly output data of each simulation. The resulting TCGI-R fields for the control (forced with climatological SST) are shown together with those computed from the NCEP and ERA40 reanalyses in Fig. 5. The climatology of the HIRAM model for the present is very similar to that of the reanalysis. The main differences are the higher values of the index in the eastern North

Pacific and South Pacific, and the shift in the location of the western North Pacific maximum northeastward, compared with the reanalysis climatology for the period 1961-2000.

Similarly, we calculated the climatologies for the future scenarios forced with SST anomalies. These are shown in Fig. 6. As might have been expected, the gross features of the climatologies are very similar, with differences in the maxima's locations and strengths in each case varying according to the SST anomaly patterns in each case.

Next we compare the future climatologies of TCGI-R with that in the present in the HIRAM simulations. The differences between them are shown in Fig. 7. While the number of TCs in all future scenarios decreases globally compared with the present, the difference in TCGI-R is positive when integrated globally, indicating that the index predicts an increase in the number of TCs. The TCGI-R index fails to predict the reduction in the number of TCs observed in the HIRAM model.

6. TCGI obtained from HIRAM model

One reason for the TCGI-R increases in the future while the NTC decreases in the same simulations could be that the index was obtained using a statistical regression between reanalysis variables and observed TCs, rather than using the model output itself to derive the index. Therefore, we repeat the TCGI fitting procedure using the HIRAM simulations of present-day climate fields and TCs. Besides the variables used in the TCGI-R, we will test various other variable combinations for our predictands. We will call the indices obtained from HIRAM data TCGI-H and will test their abilities to predict the number of future TCs in the model.

First we use the same environmental variables as in TCGI-R, i.e.: low-level vorticity, vertical wind shear, column relative humidity and relative SST (RSST). We obtained a new index, TCGI-H, with the same variables but slightly different coefficients than TCGI-R. The coefficients of TCGI-R and TCGI-H are compared in table 2. We then used the HIRAM environmental variables for this index for the control and warm scenarios. The climatological patterns are very similar to those shown in Fig. 5(a) and 6, and are not shown. The difference in the future scenarios and the control run of the TCGI-H index is shown in Fig. 8. Similarly to what we obtained when using TCGI-R, TCGI-H leads to an increase in TC activity in the HIRAM model, while there is a decrease in NTC.

Given that our first choice of predictors did not lead to the reduction of TC activity in the model, we tested various other combinations of predictors. In each case we examine the ability of the resulting index to simulate a reduction in global TC frequency in the future. Fig. 9 shows the difference of indices integrated globally in the future and in the present using various scenarios, using as predictors low-level vorticity (850hPa), vertical wind shear, and either column relative humidity (the ratio of column water vapor to its saturation value) or saturation deficit (the difference between column water vapor and its saturation value) together with either potential intensity (PI), relative SST (RSST) or total SST. All cases with the column relative humidity predict an increase in TC activity in the future, of varying magnitude from one index to the next.

Emanuel (2010) pointed out the importance of using the saturation deficit in predicting future tropical cyclone activity. When the saturation deficit is used as one of the index predictors (right panels), we obtain a reduction in future cyclone frequency for the cases in which the saturation deficit is used, in conjunction with either PI or RSST. We also show in Fig. 9 the difference of the mean global NTC in the present and the mean global NTC in the future scenarios (white bars). While the combination of both PI and RSST with saturation deficit results in a reduction of the index, amounting to a prediction of a decrease of TC activity in the future, the magnitude of the decrease is higher than that which occurs in the model-simulated NTC when RSST is a model predictor. On the other hand, the decrease in the index constructed using the combination of saturation deficit and PI is very close to the model decrease in NTC.

Using the change in the global tropical cyclone frequency in future and present as our measure for the "best" TCGI-H index, the pairing of saturation deficit and PI seems to be the best choice of those we tried. These predictors are very similar to those Emanuel (2010) used in his improved genesis potential index, although the methodologies by which the two were derived are different. However, if we apply the Emanuel (2010) index to the HIRAM environmental variables it predicts an increase in the TC activity in all scenarios (not shown), similar to what happens when using the Emanuel and Nolan (2004) original GPI (not shown).

Given that the combination of saturation deficit and PI is our best choice for predicting a reduction, we examine the spatial pattern of the difference in the future and present TCGI-H for that combination of variables (Fig. 10). While the decrease in TC activity in the future is apparent all cases in Fig. 10, the southern hemisphere, particularly the south Indian Ocean, is the location with the highest negative anomalies. We now examine whether the reduction in the frequency of storms is similarly greater in the southern hemisphere compared with the northern hemisphere. Fig. 11 shows the NTC per year in each hemisphere in future scenarios, normalized by the mean NTC per year in the control run in each hemisphere. While there is a percentage reduction overall in both Northern and Southern hemispheres, in most models the reduction is larger in the southern than then Northern hemisphere. Furthermore the only case in which there is a significant increase in the distribution of the percentage NTC in the future occurs in the Northern hemisphere (HadCM3 SST). However, the interhemispheric asymmetry seems to be larger for the index than in the simulated NTC.

a. Vertical Velocity

Held and Zhao (2011) argued that changes in genesis in the HIRAM model in different future scenarios followed changes in the mean vertical motion, reflecting changes in convective mass fluxes. Zhao and Held (2012) analyzed the changes in the frequency of TC formation in the same HIRAM simulations that we analyze here. They computed correlations between different environmental variables, individually, and percentile changes in TC frequency. The variable with the highest correlation to TC frequency in their analysis, globally and by basin, was the 500hPa pressure vertical velocity. This suggests that we should consider using 500hPa pressure vertical velocity in the index. We test here whether including 500hPa pressure vertical velocity as one of our predictors allows us to obtain a better relationship between the index and the changes in NTC in the HIRAM model.

We repeat the procedure of Tippett et al. (2011), using as predictors again low-level vorticity and vertical shear, but instead of the column relative humidity or the saturation deficit (used above), we consider the vertical velocity. In conjunction with these three predictors, we still include either the RSST, PI or SST as the fourth possible predictor.

Similarly to Fig. 9, Fig. 12 shows the globally integrated difference between the future and present for the indices obtained using the vertical velocity as one of the predictors. In all three cases, the indices obtained using the vertical velocity either either stay nearly constant increase in the global mean, implying a prediction of either almost no change or an increase in the TC frequency. None of them predicts a substantial decrease in the HIRAM TC frequency such as actually occurs in the model. For one of the cases, namely the one in which vertical velocity and RSST are the predictors, we show in Fig. 13 the pattern of the difference between future and control simulations. While there is a decrease in TCGI-H in this case in the southern hemisphere for most scenarios, in many cases there is an increase of the index in the North Pacific, which leads to an overall increase in the global index.

Vertical velocity by itself does have a correlation with percentage changes in NTC in different regions as shown in Zhao and Held (2012). However, when used in conjunction with other environmental variables in the construction of an index which is fit to the climatological spatial distribution and seasonal cycle of genesis, it is unable to simultaneously predict the changes in NTC in the HIRAM model.

b. Fewer predictors

Given that the vertical velocity by itself is a good predictor for changes in TC frequency changes, but not when used together with other predictors, we step back and check whether it is really necessary to use four predictors in deriving TCGI-H. While this was tested using reanalysis data and observations in Tippett et al. (2011), it is possible that the result in the HIRAM model might be different.

As an example, we derived 3 new TCGI-H indices, using only three predictors: vorticity, vertical shear and either vertical velocity, column relative humidity, saturation deficity or 600hPa relative humidity; i.e., we didn't include in the statistical model SST, PI or RSST. The resulting climatologies of these indices are shown in Fig. 14. We can clearly see that when one of the thermodynamical predictors (SST, RSST or PI) is omitted, it is not possible to reproduce the climatological pattern of the TC activity globally. Thus if we wish to have an index that is able to reproduce both the spatial and seasonal patterns of TC activity in the present, as well as to predict changes in future TC activity, four predictors appear to be necessary.

The differences in the globally integrated indices in future scenarios and the present using only three predictors are shown in Fig. 15. Even if our only criterion for developing the best genesis index were the ability of the index to predict future global TC activity, the three-predictor indices still fall short. Notice that when we use vertical velocity as one of the three predictors, there is an increase in the values of the index in most scenarios (Fig. 15).

c. Additional cases

All the future scenarios discussed until now were based on adding spatially and seasonally varying SST anomalies to the SST climatology as boundary condition for the HIRAM model. Two additional simulations were available to us. In the first one the historical climatological (i.e., control) SST is used, while the $\mathrm{CO_2}$ concentration in the model was doubled. We call this case $2CO_2$. In the other case, we changed the SST by adding 2K uniformly to the SST climatologies, called here plus 2K or p2K, but CO_2 was kept constant. These cases were analyzed previously in Held and Zhao (2011) and Zhao and Held (2012); those authors concluded that the changes in the TC activity in the future could be attributed to both the changes in CO_2 and to the changes in SST, with a nearly equal contribution from each factor.

Here we examine the TCGI-H predictions for these two cases. In both cases in the global NTC is reduced, as shown in Fig. 3. While the climatology of the various TCGI-H indices in the present are very similar to the other cases, and to each other, the changes in the future for these 2 scenarios are very different from what we obtained in the other scenarios.

Fig 16 shows the difference between the future and present for the $2CO_2$ scenario using many TCGI-H choices, with various combinations of predictors. Similarly, Fig 17, shows these differences for the p2K scenario. Figs. 16 and 17 are close to the opposites of each other for all panels. While the indices constructed with column relative humidity and PI predict a significant uniform increase in TC activity regions in the future for the CO_2 scenario, there is a very similar decrease in the p2K scenario. In contrast, the indices with vertical velocity show much smaller and sporadic differences, with the values of the indices slightly decreasing for the CO_2 case and slightly increasing in the p2K case. It is puzzling how different changes in the indices are in these two scenarios from the other cases examined before.

At this point, we do not have a truly satisfactory explanation for the apparent failure of our index methodology in the case of the $2CO_2$ and p2K experiments. At a somewhat superficial level, it seems that our index is more successful when changes in the environment for TCs are caused by climate change with some spatial structure, here imposed through the SST field. This is broadly consistent with arguments based on relative SST; on the other hand, such arguments might suggest that in there might be cancellation between NTC changes in different regions (since by definition relative SST cannot have the same sign everywhere). In this light, the fact that our index — if saturation deficit and PI are chosen as the thermodynamic predictors — is able to capture the global mean change in the various CMIP-based SST scenarios is encouraging. At the same time, our index fails to capture global NTC changes when the imposed forcings, whether SST or CO_2, have no spatial structure. We leave this as an open problem for future work.

7. Discussion

Genesis indices have been widely used in the climate community as a proxy for TC activity in models. Given that climate models are usually better at simulating the large-scale climate features than they are at simulating the TCs themselves, genesis indices are potentially useful for inferring TC activity in simulated present (e.g. seasonal forecasts) and future climates. However, it has been shown that the relationship of models' own TCs and genesis indices computed from the same models' large-scale fields is not optimal; a strong relationship between them occurs only in specific cases, e.g. in same basins and models (Camargo et al. 2007b). In the case of a genesis index developed for the North Atlantic, a relationship is valid only when smaller sub-basins are considered (Bruyère et al. 2012). Walsh et al. (2010) found that the agreement between one genesis index (GPI) and model TCs increased with model resolution.

Here we explored the relationship of genesis indices to the frequency of TCs in models further, using a methodology that we developed previously that allows us to derive genesis indices, easily and reproducibly, from environmental fields (from reanalysis or models) and TC frequency (from observations or models). Although all the genesis indices examined (TCGI-R, TCGI-H, GPI and new GPI) are able to reproduce the climatology of the model TC activity well, most of the genesis indices tested predict an increase of TC activity in future climates (including TCGI-R, GPI and new GPI), while the global TC frequency in the HIRAM model in these climates, similarly to other high-resolution climate models, decreases relative to the present. Only one of the combination of predictors tested, the one using PI and saturation deficit, is able to capture the reduction of the global frequency in future climates. Using fewer than four predictors, as suggested by Bruyère et al. (2012) leads to other problems, such as substantial errors in the climatological pattern.

Our primary conclusions are:

i. Many genesis indices developed for the present climatology are not able to capture the reduction of global TC activity in a warmer world, at least within the context of the HIRAM model. A successful fit to the present climatology, or even success in interannual prediction or other independent data, is not a guarantee that the index will capture the response to greenhouse gas-induced warming.

ii. Our results suggest that the global reduction in TC frequency in warmer climates simulated by the HIRAM model is attributable to the increasing saturation deficit as temperature increases while relative humidity stays close to constant. This effect is partly compensated by increases in PI, which reduce the magnitude of the decrease in TC frequency.

iii. Our results show the value of an objective and reproducible method to derive genesis indices, as derived in Tippett et al. (2011). As either new observations of TCs Landsea et al. (2008,

2012) or large-scale fields (or both) become available, or new insights emerge regarding which environmental variables are important to genesis, our methodology will allow us to derive better indices.

iv. However, our methodology fails here to capture the global TC changes found in which the forcings — either SST or CO_2 — have no spatial structure. At present, we do not understand whether this is a failure of the index methodology itself, a poor choice of predictors, or some other issue.

Acknowledgments.

This work was supported in part by NOAA grants NA08OAR4320912 and NA11OAR4300193, NSF grant AGS 1143959 and ONR grant N00014-12-1-0911.

REFERENCES

Bell, R., J. Strachan, P. L. Vidale, K. Hodges, and M. Roberts, 2013: Response of tropical cyclones to idealized climate change experiments in a global high resolution coupled general circulation model. *J. Climate*, doi:10.1175/JCLI-D-12-00749.1, in press.

Bengtsson, L., H. Böttger, and M. Kanamitsu, 1982: Simulation of hurricane-type vortices in a general circulation model. *Tellus*, **34**, 440–457.

Bruyère, C. L., G. J. Holland, and E. Towler, 2012: Investigating the use of a genesis potential index for tropical cyclones in the north atlantic basin. *J. Climate*, **25**, 8611–8626.

Bye, J. and K. Keay, 2008: A new hurricane index for the Caribbean. *Interscience*, **33**, 556–560.

Camargo, S. J., 2013: Global and regional aspects of tropical cyclone activity in the CMIP5 models. *J. Climate*, doi:10.1175/JCLI-D-12-00549.1, in press.

Camargo, S. J., A. G. Barnston, and S. E. Zebiak, 2005: A statistical assessment of tropical cyclones in atmospheric general circulation models. *Tellus*, **57A**, 589–604.

Camargo, S. J., H. Li, and L. Sun, 2007a: Feasibility study for downscaling seasonal tropical cyclone activity using the NCEP regional spectral model. *Int. J. Clim.*, **27**, 311–325, doi: 10.1002/joc.1400.

Camargo, S. J., A. H. Sobel, A. G. Barnston, and K. A. Emanuel, 2007b: Tropical cyclone genesis potential index in climate models. *Tellus*, **59A**, 428–443.

Camargo, S. J., M. C. Wheeler, and A. H. Sobel, 2009: Diagnosis of the MJO modulation of tropical cyclogenesis using an empirical index. *J. Atmos. Sci.*, **66**, 3061–3074.

Delworth, T. L., et al., 2012: Simulated climate and climate change in the GFDL CM2.5 high-resolution coupled climate model. *J. Climate*, **25**, 2755–2781.

DeMaria, M., J. A. Knaff, and B. H. Conell, 2001: A tropical cyclone genesis parameter for the tropical Atlantic. *Wea. Forecasting*, **16**, 219–233.

Emanuel, K., 2006: Climate and tropical cyclone activity: A new model downscaling approach. *J. Climate*, **19**, 4797–4802.

Emanuel, K., 2010: Tropical cyclone activity downscaled from NOAA-CIRES reanalysis, 1908-1958. *J. Adv. Model. Earth Syst.*, **2**, doi:10.3894/JAMES.2010.2.1.

Emanuel, K., S. Ravela, E. Vivant, and C. Risi, 2006: A statistical deterministic approach to hurricane risk assessment. *Bull. Amer. Meteor. Soc.*, **87**, 299–314.

Emanuel, K. A., 2013: Downscaling CMIP5 climate models shows increased tropical cyclone activity over the 21st century. *Proc. Nat. Acad. Sci.*, **110**, doi:10.1073/pnas.1301293110.

Emanuel, K. A. and D. S. Nolan, 2004: Tropical cyclone activity and global climate. *Proc. of 26th Conference on Hurricanes and Tropical Meteorology*, Miami, FL, American Meteorological Society, 240–241.

Gray, W. M., 1979: *Meteorology over the tropical oceans*, chap. Hurricanes: Their formation, structure and likely role in the tropical circulation, 155–218. Roy. Meteor. Soc.

Held, I. M. and M. Zhao, 2011: The response of tropical cyclone statistics to an increase in CO_2 with fixed sea surface temperatures. *J. Climate*, **20**, 5353–5364.

JTWC, 2013: Joint Typhoon Warning Center Tropical Cyclone Best Track Data Site. Joint Typhoon Warning Center, Available online at http://www.npmoc.navy.mil.

Kaike, H., 1973: Information theory and an extension of the maximum likelihood principle. *2nd International Symposium on Information Theory*, B. N. Petrov and F. Czáki, Eds., Akademiai Kiadó, 267–281.

Kalnay, E., et al., 1996: The NCEP/NCAR 40-year reanalysis project. *Bull. Amer. Meteor. Soc.*, **77**, 437–441.

Kim, H.-S., G. A. Vecchi, T. Knutson, W. G. Anderson, T. L. Delworth, A. Rosati, F. Zeng, and M. Zhao, 2013: Tropical cyclone simulation and response to CO2 doubling in the GFDL CM2.5 high-resolution coupled climate model. *J. Climate*, submitted.

Kistler, R., et al., 2001: The NCEP-NCAR 50-Year reanalysis: Monthly means CD-ROM and documentation. *Bull. Amer. Meteor. Soc.*, **82**, 247–267.

Knutson, T. R., J. J. Sirutis, S. T. Garner, and R. E. T. I. M. Held, 2007: Simulation of the recent multidecadal increase of Atlantic hurricane activity using an 18-km-grid regional model. *Bull. Amer. Meteor. Soc.*, **88**, 15491565.

Knutson, T. R., J. J. Sirutis, S. T. Garner, G. A. Vecchi, and I. M. Held, 2008: Simulated reduction in atlantic hurricane frequency under twenty-first-century warming conditions. *Nature Geoscience*, **1**, 359–364.

Knutson, T. R., et al., 2010: Tropical cyclones and climate change. *Nature Geoscience*, **3**, 157–163, doi:10.1038/ngeo779.

Kotal, S. D., P. K. Kundu, and S. K. R. Bhowmik, 2009: Analysis of cyclogenesis parameter for developing and nondeveloping low-pressure systems over the indian sea. *Nat. Hazards*, **50**, 389–402.

Landman, W. A., A. Seth, and S. J. Camargo, 2005: The effect of regional climate model domain choice on the simulation of tropical cyclone-like vortices in the southwestern indian ocean. *J. Climate*, **18**, 1263–1274.

Landsea, C. W., S. Feuer, A. H. adn D. A. Glenn, J. Sims, R. Perez, M. Chenoweth, and N. Anderson, 2012: A reanalysis of the 1921-30 Atlantic hurricane database. *J. Climate*, **25**, 865–885.

Landsea, C. W., et al., 2008: A reanalysis of the 1911-20 Atlantic hurricane database. *J. Climate*, **21**, 2138–2168.

Lyon, B. and S. J. Camargo, 2009: The seasonally-varying influence of ENSO on rainfall and tropical cyclone activity in the Philippines. *Clim. Dyn*, **32**, 125 – 141, doi:10.1007/s00382-008-0380-z.

Menkes, C. E., M. Lengaigne, P. Marchesiello, N. C. Jourdain, E. M. Vincent, J. Lefèvre, F. Chauvin, and J.-F. Royer, 2012: Comparison of tropical cyclonegenesis indices on seasonal to interannual timescales. *Clim. Dyn.*, **38**, 301–321.

Murakami, H. and B. Wang, 2010: Future change of north atlantic tropical cyclone tracks: Projection by a 20-km-mesh global atmospheric model. *J. Climate*, **23**, 2569–2584, doi: 10.1175/2010JCLI3338.1.

NHC, 2013: NHC (National Hurricane Center) best track dataset. National Hurricane Center, available online at http://www.nhc.noaa.gov, available online at http://www.nhc.noaa.gov.

Nolan, D. S., E. D. Rappin, and K. A. Emanuel, 2007: Tropical cyclogenesis sensitivity to environmental parameters in radiative-convective equilibrium. *Q. J. R. Meteorol. Soc*, **133**, 2085–2107.

Ramsay, H. A. and A. H. Sobel, 2011: The effects of relative and absolute sea surface temperature on tropical cyclone potential intensity using a single column model. *J. Climate*, **24**, 183–193.

Roberts, M. J., et al., 2009: Impact of resolution on the tropical Pacific circulation in a matrix of coupled models. *J. Climate*, **22**, 2541–2556.

Royer, J.-F., F. Chauvin, B. Timbal, P. Araspin, and D. Grimal, 1998: A GCM study of the impact of greenhouse gas increase on the frequency of occurrence of tropical cyclone. *Clim. Change*, **38**, 307–343.

Sall, S. M., H. Sauvageot, A. T. Gaye, A. Viltard, and P. de Felice, 2006: A cyclogenesis index for tropical Atlantic off the African coasts. *Atmospheric Research*, **79**, 123–147.

Swanson, K. L., 2008: Nonlocality of atlantic tropical cyclone intensity. *Geochem. Geophys. Geosyst.*, **9**, Q04V01.

Tippett, M. K., S. J. Camargo, and A. H. Sobel, 2011: A Poisson regression index for tropical cyclone genesis and the role of large-scale vorticity in genesis. *J. Climate*, **24**, 2335–2357.

Tippett, M. K., A. H. Sobel, and S. J. Camargo, 2012: Association of monthly u.s. tornado occurrence with large-scale atmospheric parameters. *Geophys. Res. Lett.*, **39**, L02 801, doi: 10.1175/2011GL050368.

Uppala, S. M., et al., 2005: The ERA-40 re-analysis. *Quart. J. Roy. Meteor. Soc.*, **131**, 2961–3012, doi:10.1256/qj.04.176.

Vecchi, G. A. and B. J. Soden, 2007: Effect of remote sea surface temperature change on tropical cyclone potential intensity. *Nature*, **450**, 1066–1070, doi:10.1038/nature06423.

Vecchi, G. A., M. Zhao, H. Wang, G. Villarini, A. Rosati, A. Kumar, K. M. Held, and R. Gudgel, 2011: Statististical-dynamical predictions of seasonal north atlantic hurricane activity. *Mon. Wea. Rev.*, **139**, 1070–1082.

Villarini, G. and G. A. Vecchi, 2012: Twenty-first-century projections of north atlantic tropical storms from cmip5 models. *Nature Clim. Change*, **2**, 604–607.

Villarini, G. and G. A. Vecchi, 2013: Projected increases in north atlantic tropical cyclone intensity from cmip5 models. *J. Climate*, doi:JCLI-D-12-00441.1, in press.

Vitart, F., D. Anderson, and T. Stockdale, 2003: Seasonal forecasting of tropical cyclone landfall over Mozambique. *J. Climate*, **16**, 3932–3945.

Vitart, F., J. L. Anderson, and W. F. Stern, 1997: Simulation of interannual variability of tropical storm frequency in an ensemble of GCM integrations. *J. Climate*, **10**, 745–760.

Walsh, K., S. Lavender, H. Murakami, E. Scoccimarro, L.-P. Caron, and M. Ghantous, 2010: *The tropical cyclone climate model intercomparison*, Hurricanes and Climate Change, Vol. 2, chap. 1, 1–23. Springer Verlag.

Walsh, K., S. Lavender, E. Scoccimarro, and H. Murakami, 2013: Resolution dependence of tropical cyclone formation in cmip3 and finer resolution models. *Clim. Dyn.*, **40**, 585–599.

Yokoi, S. and Y. N. Takayabu, 2009: Multi-model projection of global warming impact on tropical cyclone genesis frequency over the western North Pacific. *J. Meteor. Soc. Japan*, **87**, 525–538.

Yokoi, S., Y. N. Takayabu, and J. C. L. Chan, 2009: Tropical cyclone genesis frequency over the western North Pacific simulated in medium-resolution coupled general circulation models. *Clim. Dyn.*, **33**, 665–683.

Zhao, M. and I. M. Held, 2010: An analysis of the effect of global warming on the intensity of atlantic hurricanes using a GCM with statistical refinement. *J. Climate*, **23**, 6382–6393.

Zhao, M. and I. M. Held, 2012: TC-Permitting GCM simulations of hurricane frequency response to sea surface temperature anomalies projected for the late-twenty-first century. *J. Climate*, **25**, 2995–3009.

Zhao, M., I. M. Held, S.-J. Lin, and G. A. Vecchi, 2009: Simulations of global hurricane climatology, interannual variability and response to global warming using a 50 km resolution gcm. *J. Climate*, **22**, 66536678.

Zhao, M., I. M. Held, and G. A. Vecchi, 2010: Retrospective forecasts of the hurricane season using a global atmospheric model assuming persistence of SST anomalies. *Mon. Wea. Rev.*, **138**, 3858–3868.

List of Tables

1	HIRAM simulations used in this study: forcing, name, duration	27
2	Coefficients of the Poisson regression between the numbers of tropical cyclone genesis (TCG) events for the reanalsyis index (TCGI-R) and the HIRAM index (TCGI-H)	28

TABLE 1. HIRAM simulations used in this study: forcing, name, duration

Type	Name	Duration
Climatological SST	Clim	25 years
Multi-model ensemble mean SST anomalies	Warm	20 years
SST anomalies CCCMA model	CCCMA	10 years
SST anomalies Echam5 model	Echam5	10 years
SST anomalies GFDL CM2.1 model	GFDL 2.1	10 years
SST anomalies GFDL CM2.0 model	GFDL 2.0	10 years
SST anomalies HadCM3 model	HadCM3	10 years
SST anomalies HadGEM1 model	HadGEM1	10 years
SST anomalies MIROC model	MIROC	10 years
SST anomalies MRI model	MRI	10 years
2 times CO_2	CO2	20 years
SST plus 2K globally	p2K	20 years

TABLE 2. Coefficients of the Poisson regression between the numbers of tropical cyclone genesis (TCG) events for the reanalsyis index (TCGI-R) and the HIRAM index (TCGI-H)

Index	Vorticity	Humidity	Relative SST	Shear	Constant
TCGI-R	1.12	0.12	0.46	-0.13	-11.96
TCGI-H	1.43	0.11	0.55	-0.12	-33.41

List of Figures

1 First position density and tracks for the control simulation of HIRAM (a) and (b) and in observations (c) and (d). The control simulation is forced with climatological SST for 25 years and the observed data used is for the period 1981-2005. 32

2 Mean NTC per month for the HIRAM control run and observations (1981-2005) in the (a) Southern and (b) Northern hemispheres, (c) South Indian Ocean, (d) Australian region, (e) western North Pacific and (f) North Atlantic. 33

3 Global number of TCs per year in each of the HIRAM simulations 34

4 Difference in the first position climatology between the future HIRAM simulations with different SST anomalies and the present. 35

5 Climatology of reanalysis TCGI for (a) HIRAM Clim, (b) NCEP reanalysis, (c) ERA40 reanalysis. 36

6 Climatology of TCGI-R for HIRAM runs forced with different SST anomalies as described in Table 1. 37

7 Difference in the climatology of TCGI-R for the future simulations with different SST anomalies and the present control simulation, using as TCGI-R predictors: vorticity, vertical shear, column relative humidity and RSST. 38

8 Difference in the climatology of TCGI-H for the future simulations with different SST anomalies and the present control simulation, using as TCGI-H predictors: vorticity, vertical shear, column relative humidity and RSST. 39

9 Difference of globally integrated indices (black bars) in the future (all warm scenarios) and the control simulation, using as predictors low-level vorticity, vertical wind shear, column relative humidity (left panels) or saturation deficit (right panels) and either potential intensity (PI; top panels), relative SST (RSST; middle panels) or SST (bottom panels). Difference of mean global NTC in future scenarios and present climatology for HIRAM (white bars). Scenarios are shown in the plots W (Warm), WC (Warm CCMA), WE (Warm Echam5), WG (Warm GFDL CM2.1), W0 (Warm GFDL CM2.0), W3 (Warm HadGM3), W1 (Warm HadGEM1), WO (Warm MIROC), WI (Warm MRI). 40

10 Difference in the climatology of TCGI-H for the future simulations with different SST anomalies and the present control simulation, using as TCGI-H predictors: vorticity, vertical shear, saturation deficit and potential intensity. 41

11 Box plot of NTC per year (southern hemispehre July to June season) in future scenarios normalized by the mean NTC per hemisphere in the control run in the southern (a) and northern (b) hemisphere. 42

12 Difference of globally integrated indices (black bars) in the future (all warm scenarios) and the control simulation, using as predictors low-level vorticity, vertical wind shear,vertical velocity and either potential intensity (PI; top panel), relative SST (RSST; middle panel) or SST (bottom panel). Labels of scenarios as in Fig. 9. 43

13 Difference in the climatology of TCGI-H for the future simulations with different SST anomalies and the present control simulation, using as TCGI-H predictors: vorticity, vertical shear, vertical velocity and RSST. 44

14 Climatology of TCGI-H in the present control simulation, using as TCGI-H predictors: vorticity, vertical shear, and either: column relative humidity, 600hPa relative humidity, saturation deficit, or vertical velocity. 45

15 Difference of globally integrated indices (black bars) in the future (all warm scenarios) and the control simulation, using as predictors low-level vorticity, vertical wind shear, and either (a) column relative humidity, (b) 600hPa relative humidtiy, (c) saturation deficity, (d) vertical velocity. Labels of scenarios as in Fig. 9. 46

16 Difference in the climatology of TCGI-H for the future simulations with double CO_2 and the present control simulation, using as TCGI-H predictors: vorticity, vertical shear, column relative humidity (top panels), saturation deficit (middle panels) or vertical velocity (bottom panels), as well as potential intensity (left panels) or RSST (right panels). 47

17 Difference in the climatology of TCGI-H for the future simulations with 2K added uniformily to the SST (plus 2K) and the present control simulation, using as TCGI-H predictors: vorticity, vertical shear, column relative humidity (top panels), saturation deficit (middle panels) or vertical velocity (bottom panels), as well as potential intensity (left panels) or RSST (right panels) 48

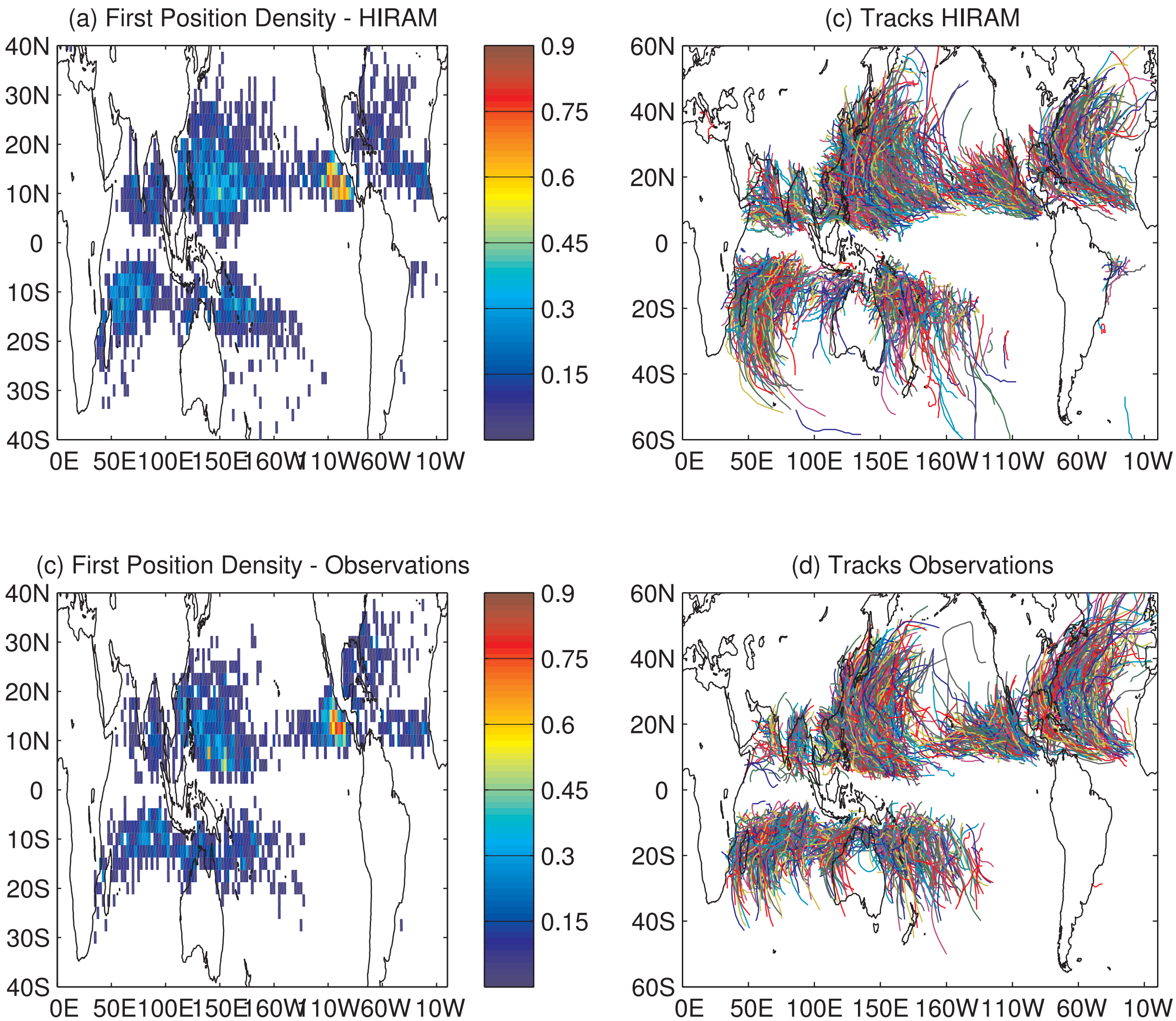

FIG. 1. First position density and tracks for the control simulation of HIRAM (a) and (b) and in observations (c) and (d). The control simulation is forced with climatological SST for 25 years and the observed data used is for the period 1981-2005.

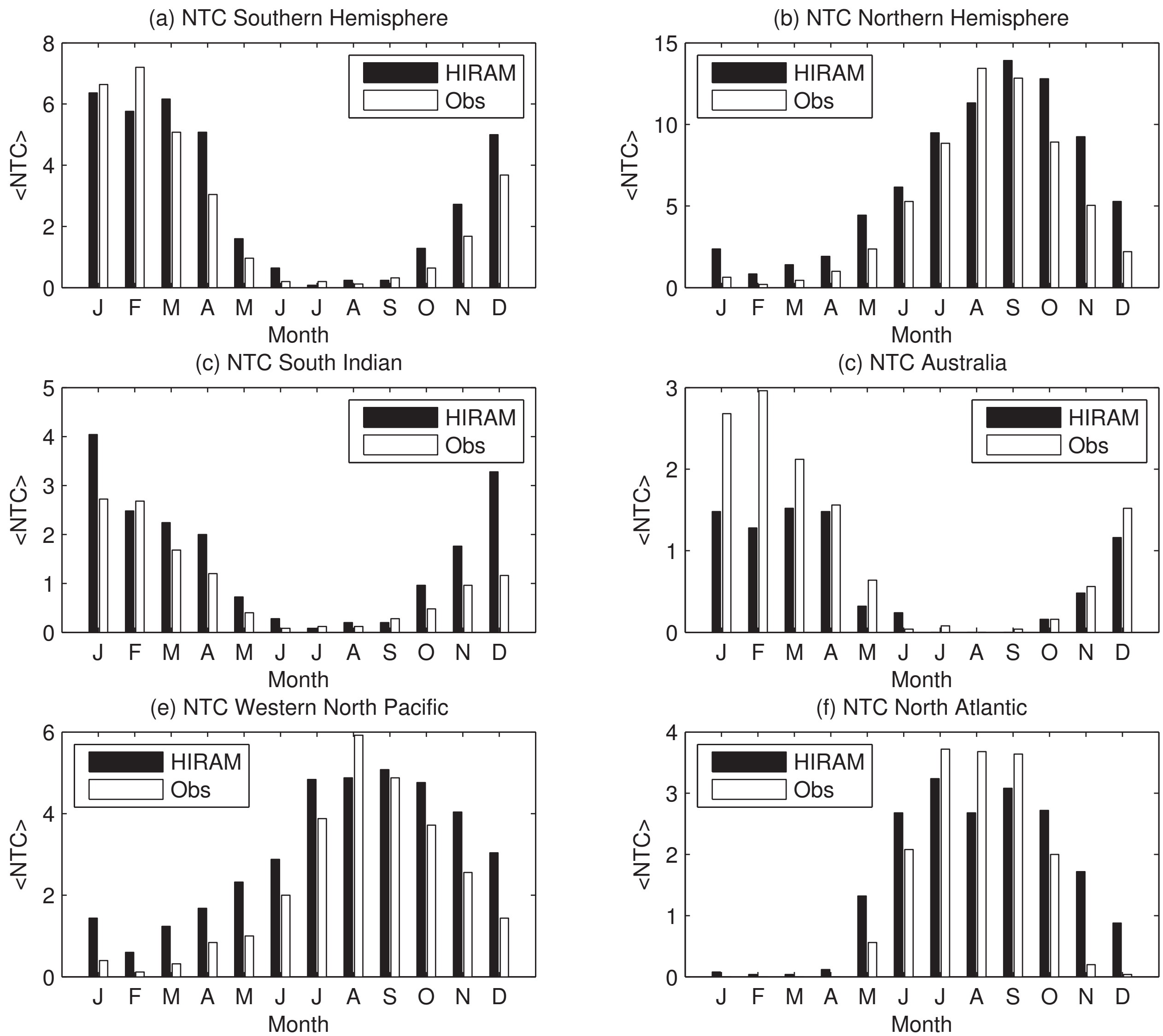

FIG. 2. Mean NTC per month for the HIRAM control run and observations (1981-2005) in the (a) Southern and (b) Northern hemispheres, (c) South Indian Ocean, (d) Australian region, (e) western North Pacific and (f) North Atlantic.

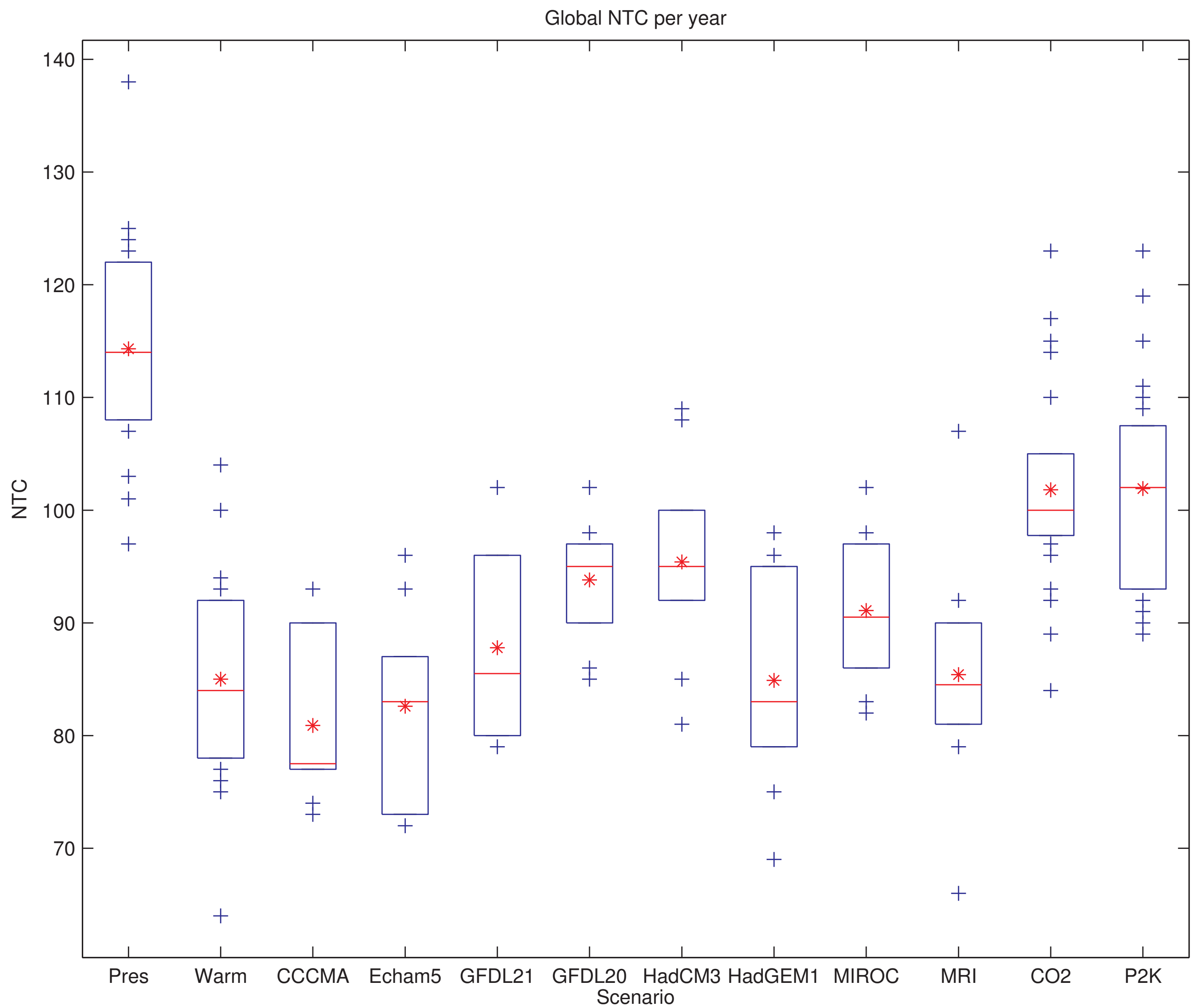

FIG. 3. Global number of TCs per year in each of the HIRAM simulations

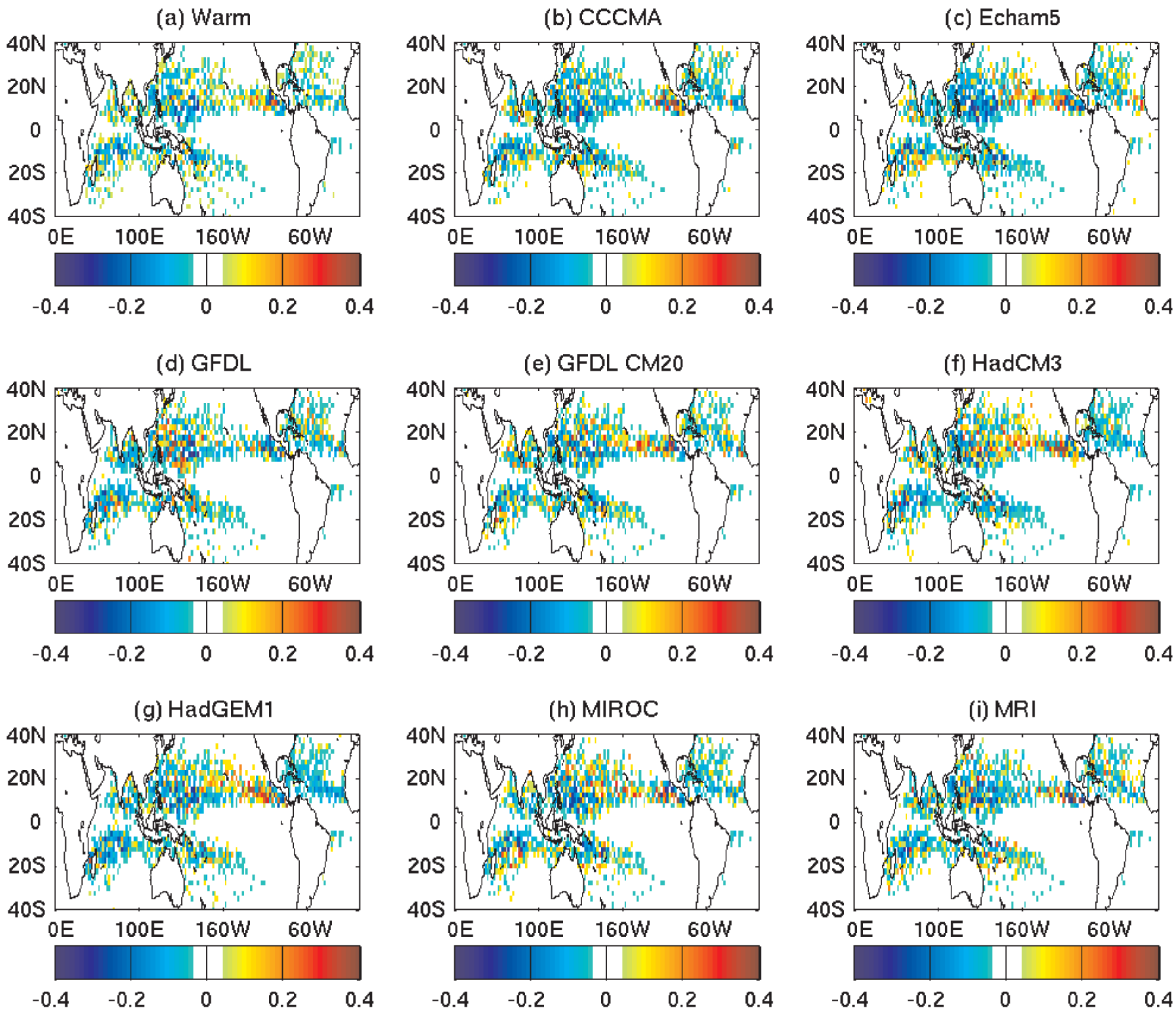

FIG. 4. Difference in the first position climatology between the future HIRAM simulations with different SST anomalies and the present.

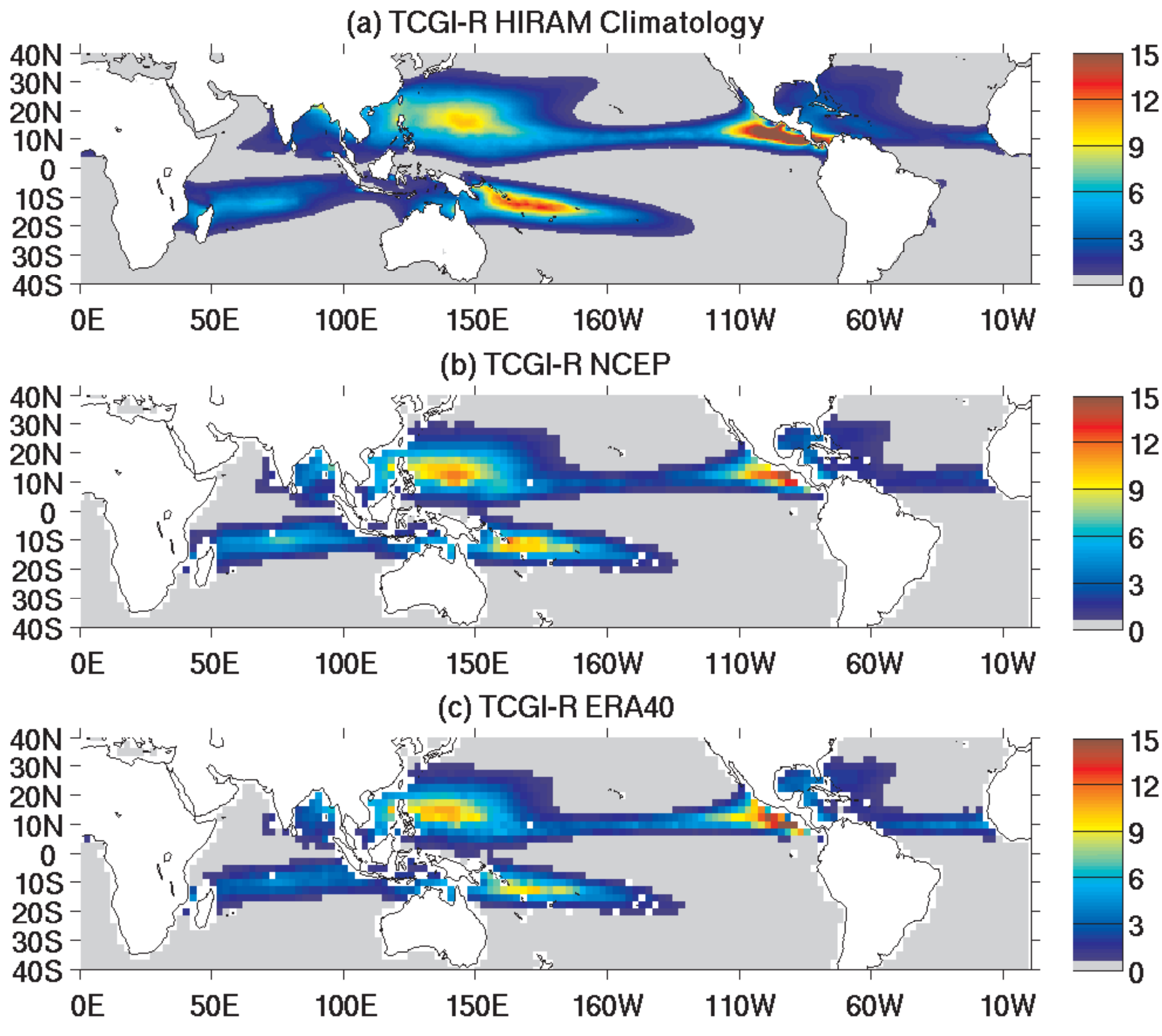

FIG. 5. Climatology of reanalysis TCGI for (a) HIRAM Clim, (b) NCEP reanalysis, (c) ERA40 reanalysis.

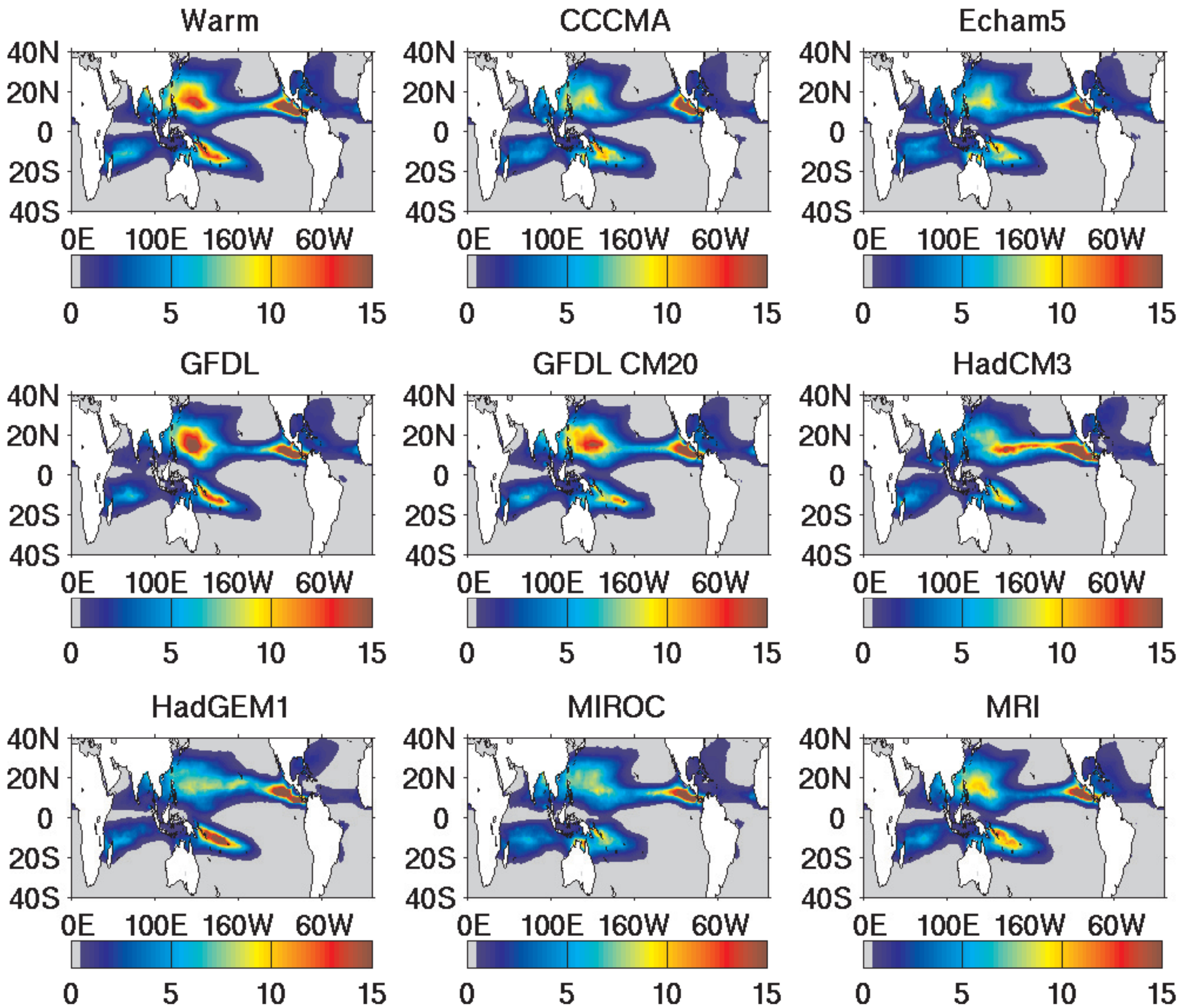

FIG. 6. Climatology of TCGI-R for HIRAM runs forced with different SST anomalies as described in Table 1.

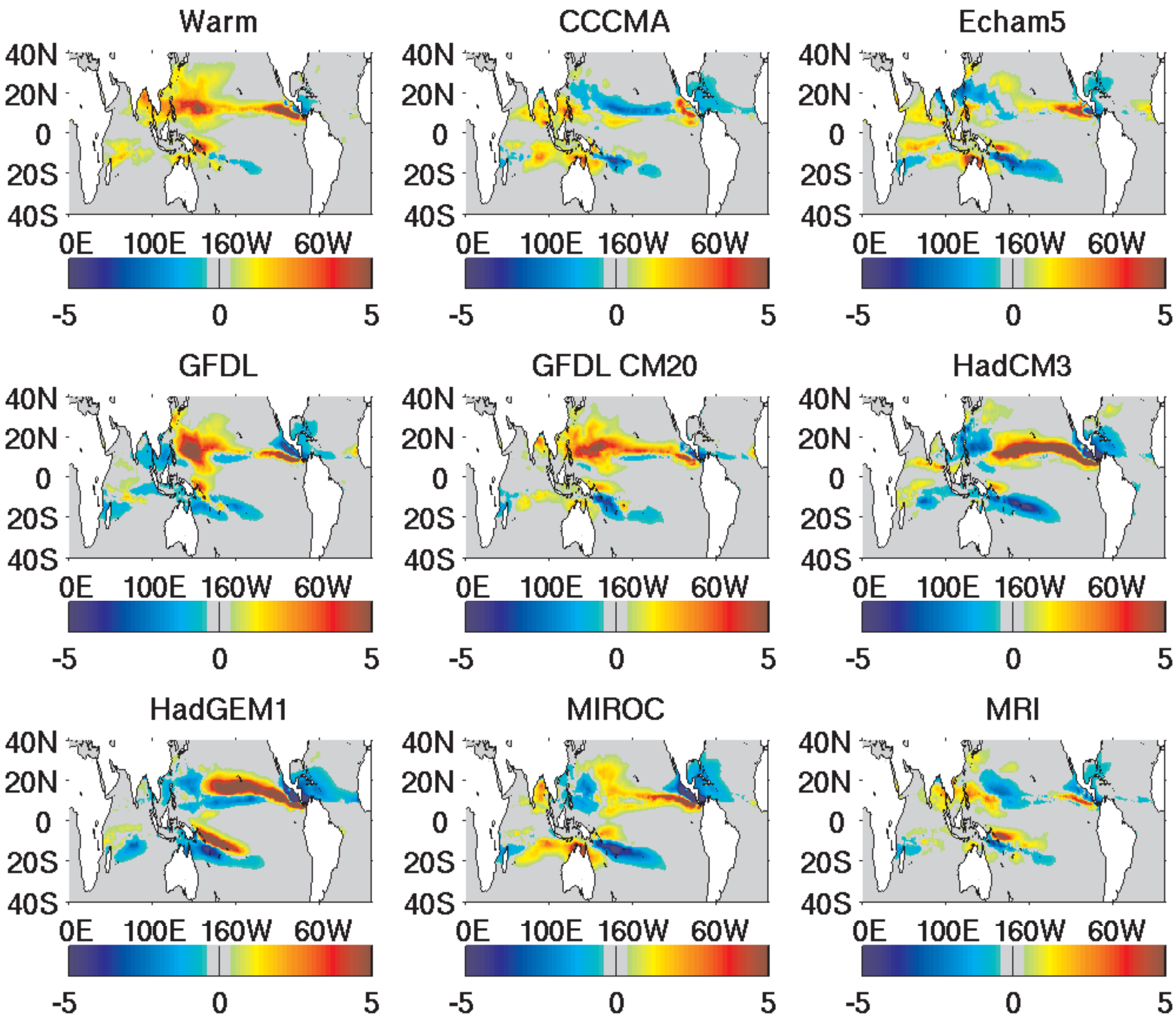

FIG. 7. Difference in the climatology of TCGI-R for the future simulations with different SST anomalies and the present control simulation, using as TCGI-R predictors: vorticity, vertical shear, column relative humidity and RSST.

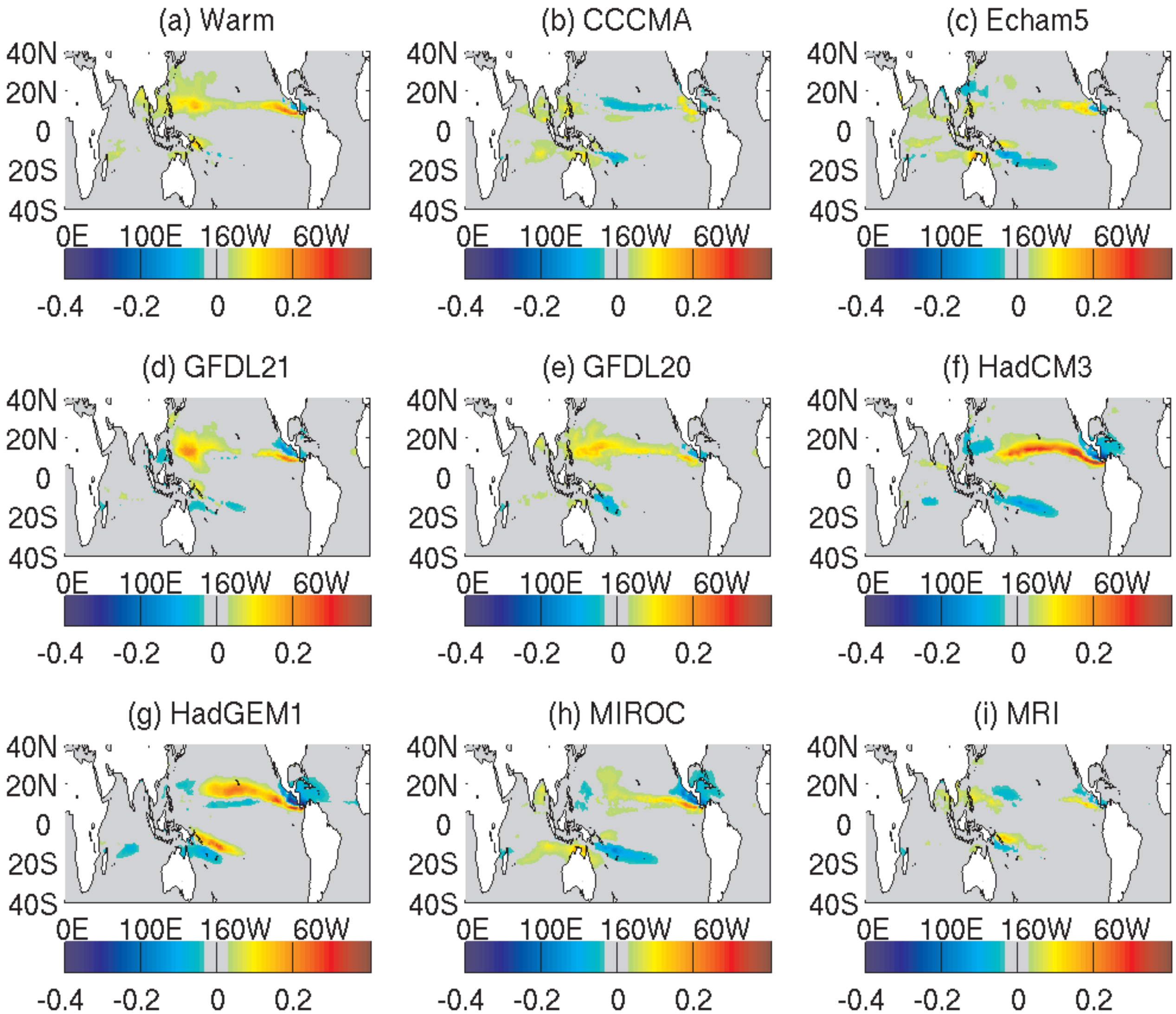

FIG. 8. Difference in the climatology of TCGI-H for the future simulations with different SST anomalies and the present control simulation, using as TCGI-H predictors: vorticity, vertical shear, column relative humidity and RSST.

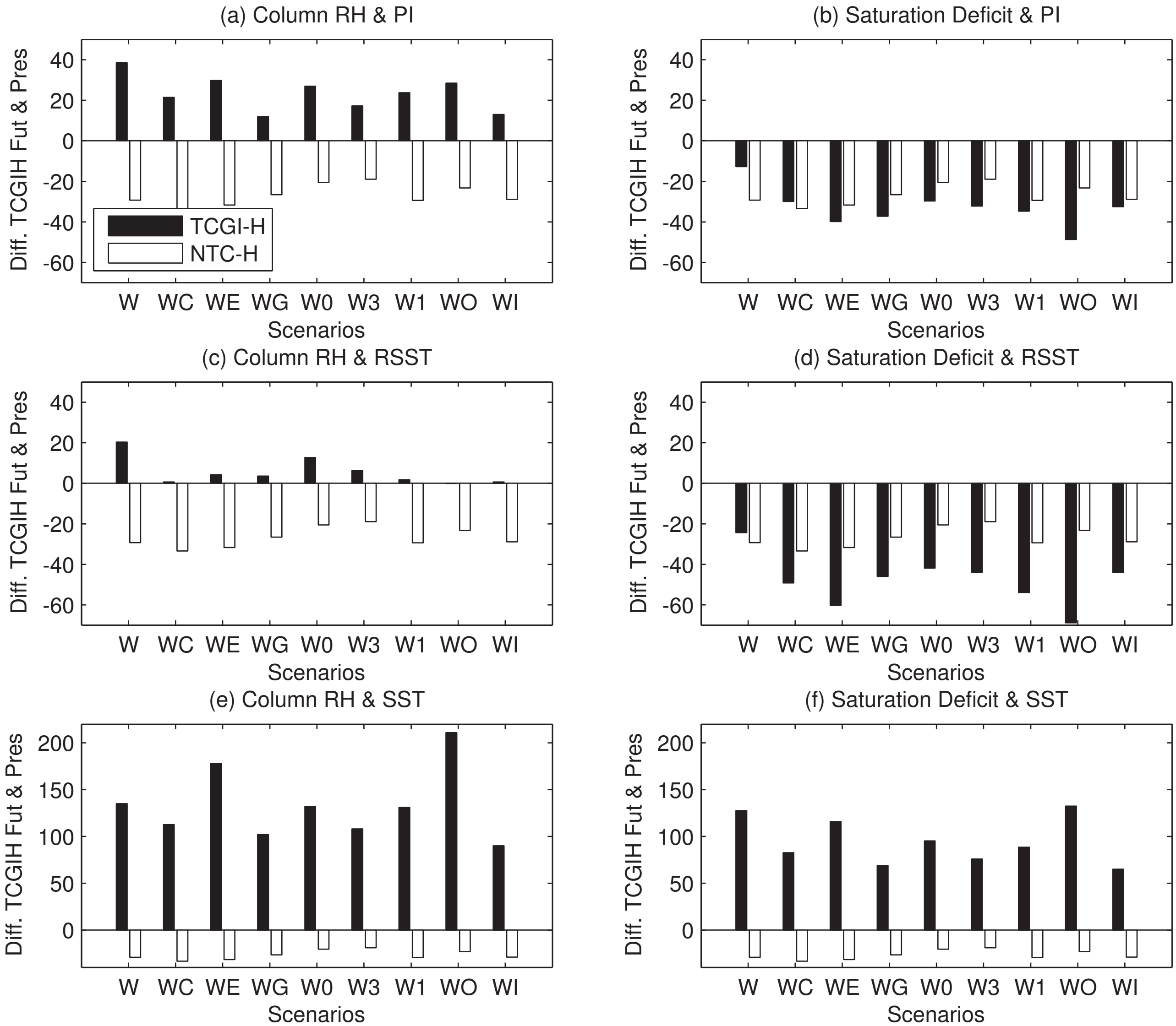

FIG. 9. Difference of globally integrated indices (black bars) in the future (all warm scenarios) and the control simulation, using as predictors low-level vorticity, vertical wind shear, column relative humidity (left panels) or saturation deficit (right panels) and either potential intensity (PI; top panels), relative SST (RSST; middle panels) or SST (bottom panels). Difference of mean global NTC in future scenarios and present climatology for HIRAM (white bars). Scenarios are shown in the plots W (Warm), WC (Warm CCMA), WE (Warm Echam5), WG (Warm GFDL CM2.1), W0 (Warm GFDL CM2.0), W3 (Warm HadGM3), W1 (Warm HadGEM1), WO (Warm MIROC), WI (Warm MRI).

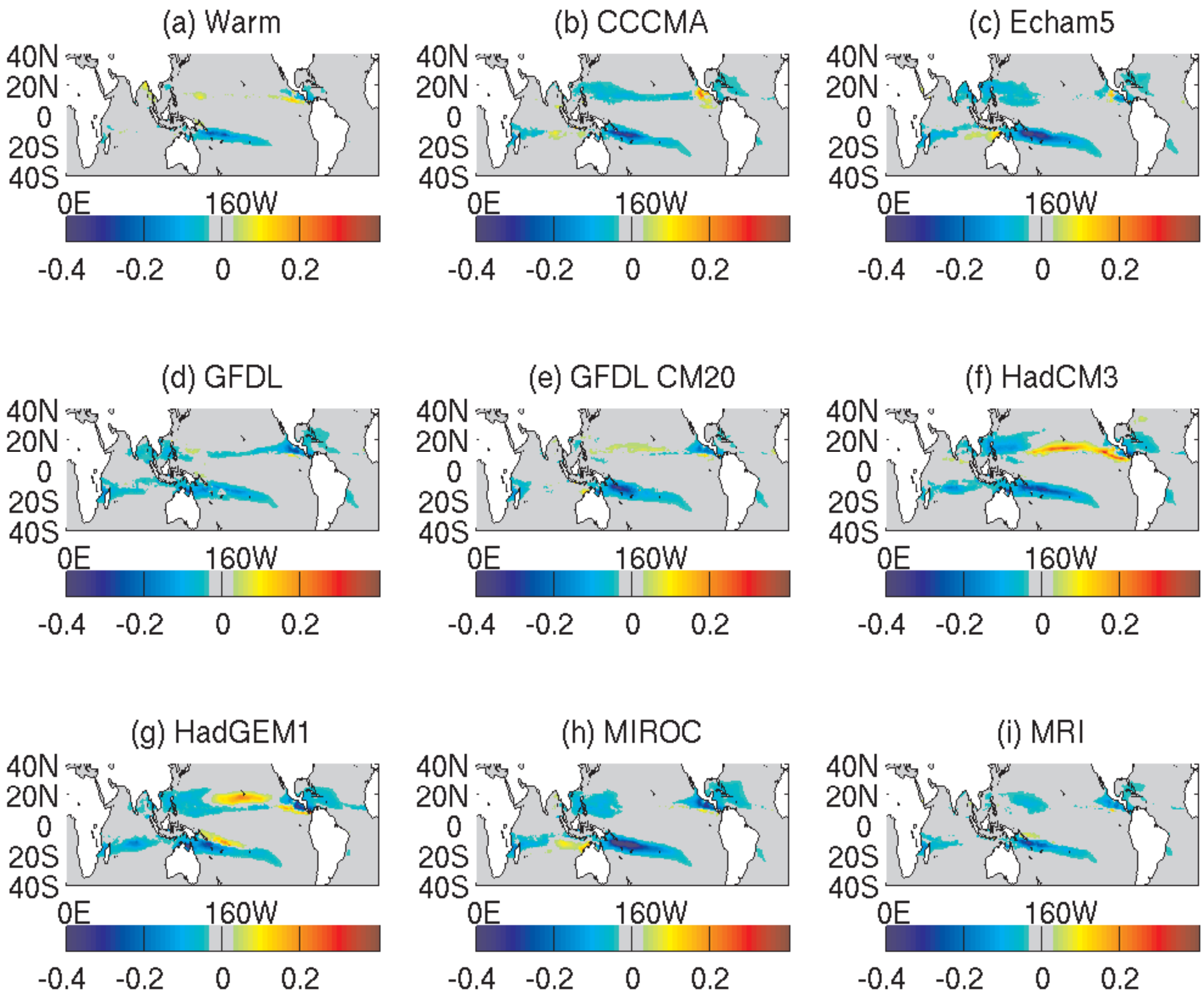

FIG. 10. Difference in the climatology of TCGI-H for the future simulations with different SST anomalies and the present control simulation, using as TCGI-H predictors: vorticity, vertical shear, saturation deficit and potential intensity.

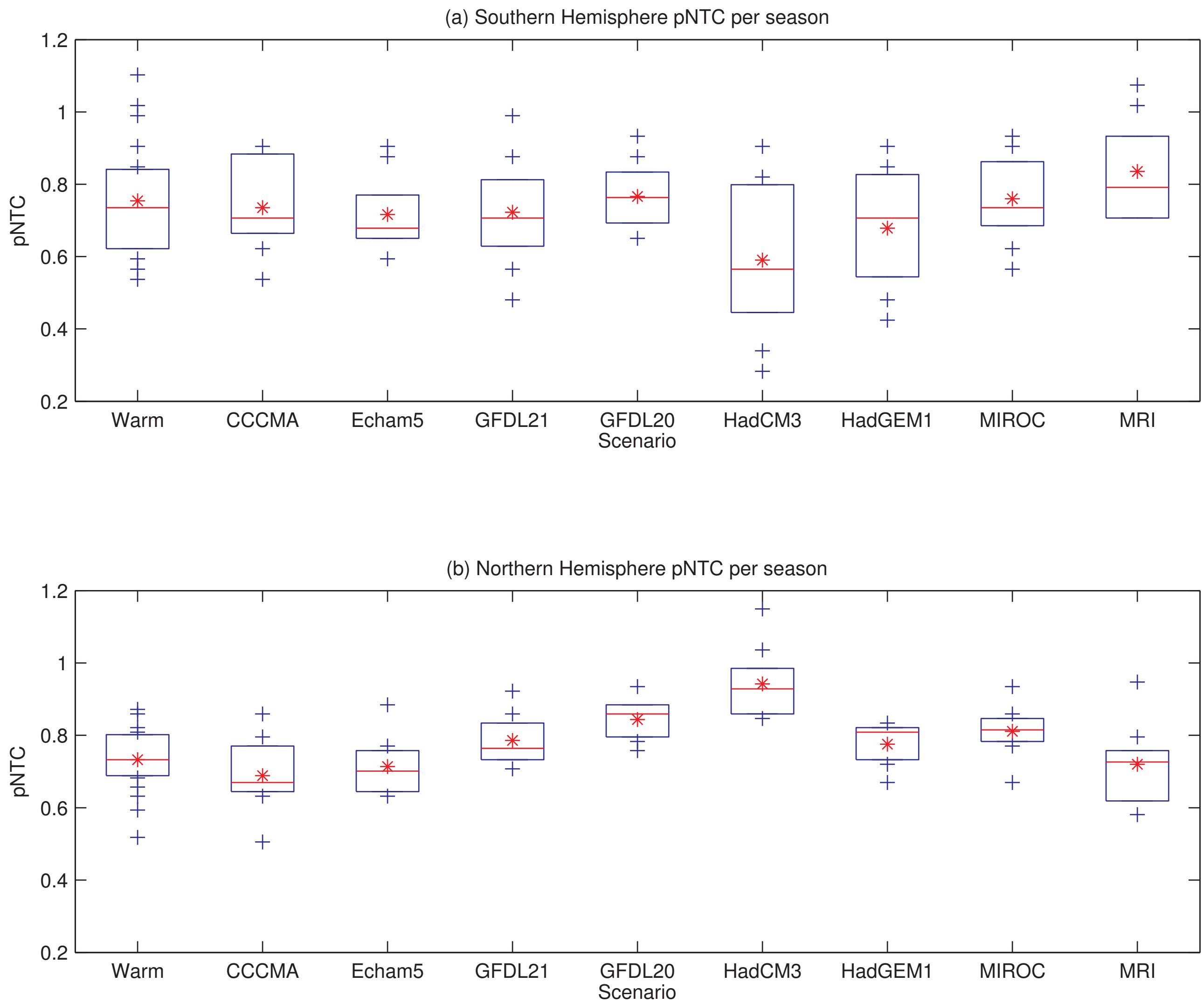

FIG. 11. Box plot of NTC per year (southern hemispehre July to June season) in future scenarios normalized by the mean NTC per hemisphere in the control run in the southern (a) and northern (b) hemisphere.

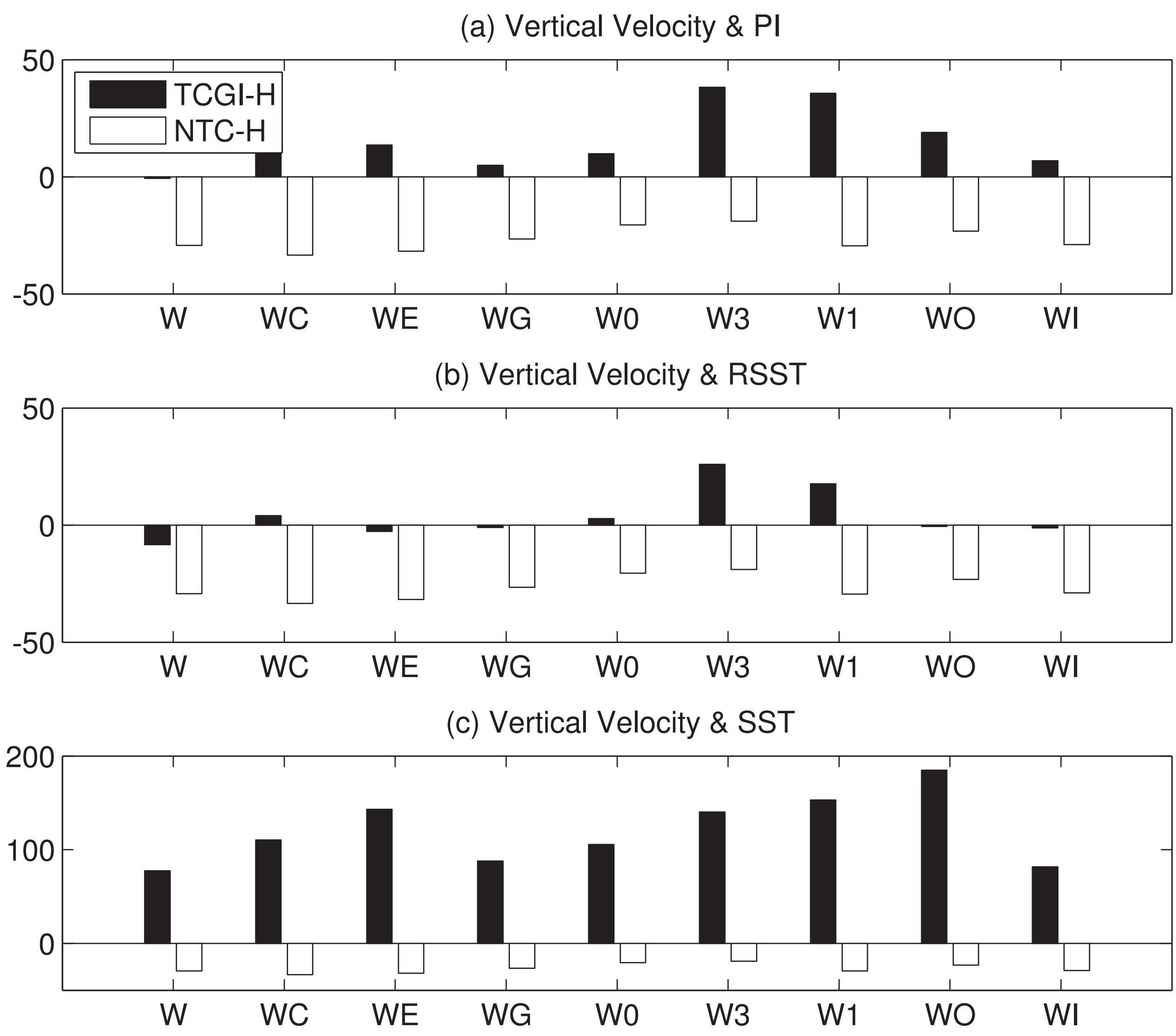

FIG. 12. Difference of globally integrated indices (black bars) in the future (all warm scenarios) and the control simulation, using as predictors low-level vorticity, vertical wind shear,vertical velocity and either potential intensity (PI; top panel), relative SST (RSST; middle panel) or SST (bottom panel). Labels of scenarios as in Fig. 9.

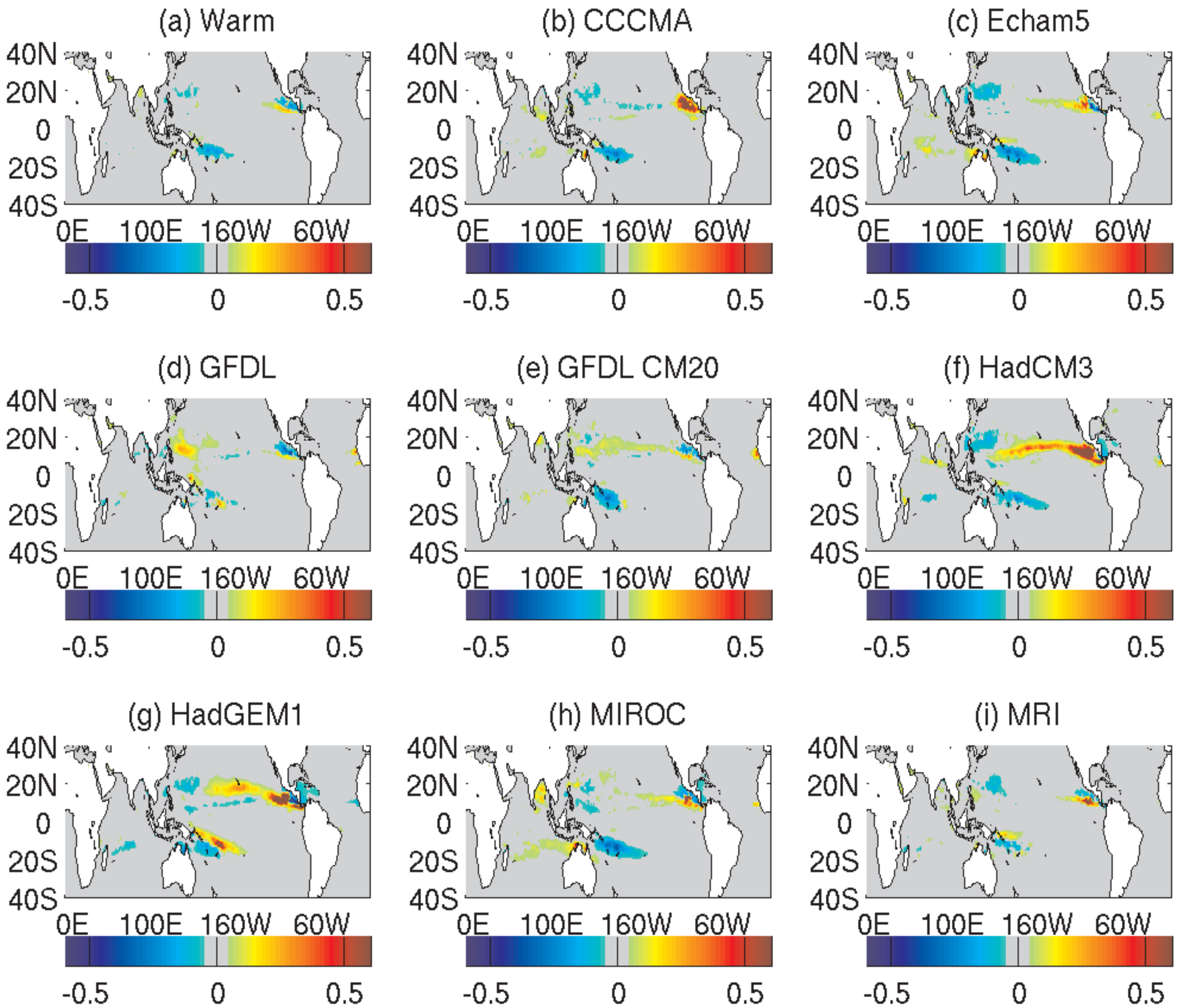

FIG. 13. Difference in the climatology of TCGI-H for the future simulations with different SST anomalies and the present control simulation, using as TCGI-H predictors: vorticity, vertical shear, vertical velocity and RSST.

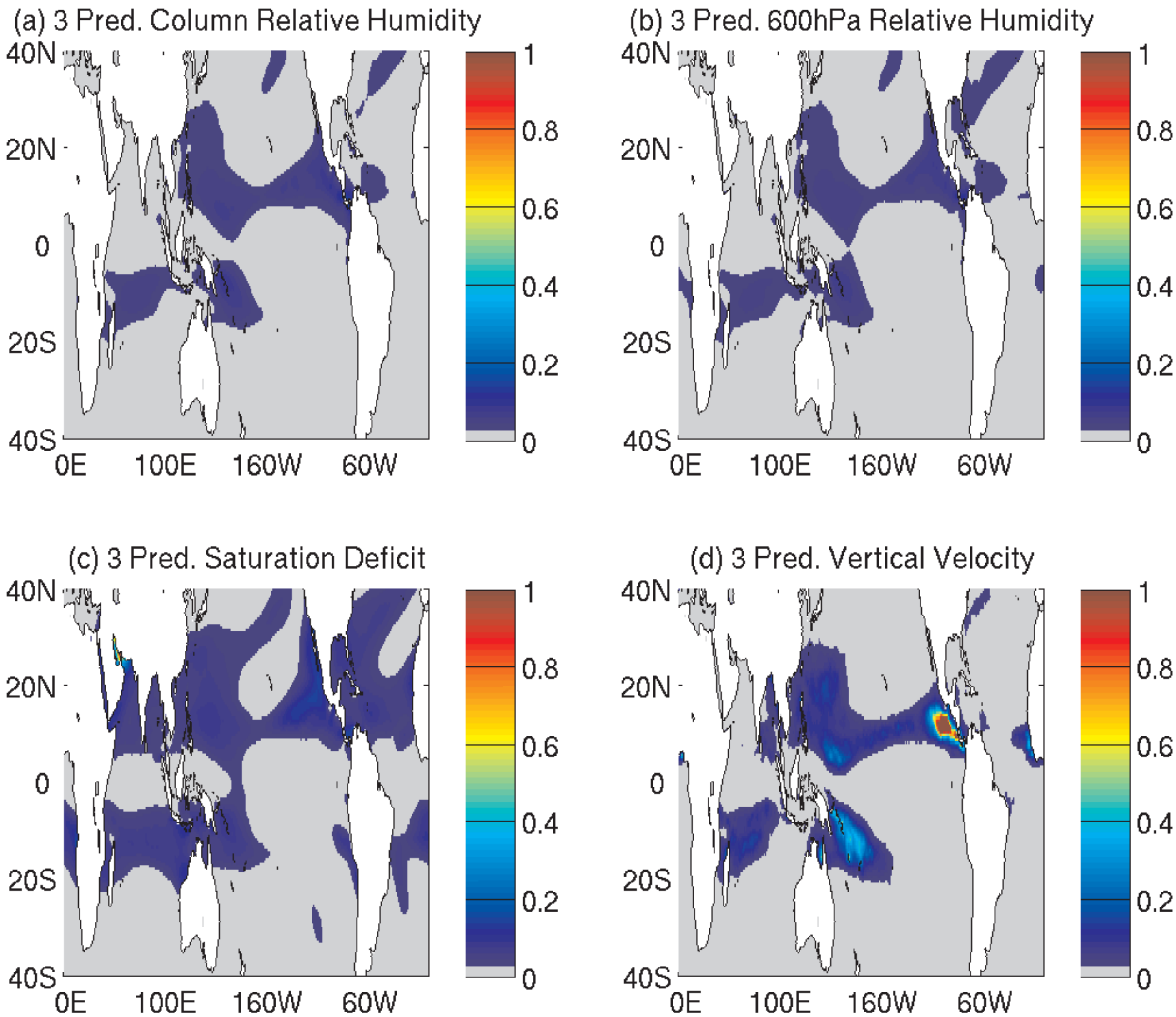

FIG. 14. Climatology of TCGI-H in the present control simulation, using as TCGI-H predictors: vorticity, vertical shear, and either: column relative humidity, 600hPa relative humidity, saturation deficit, or vertical velocity.

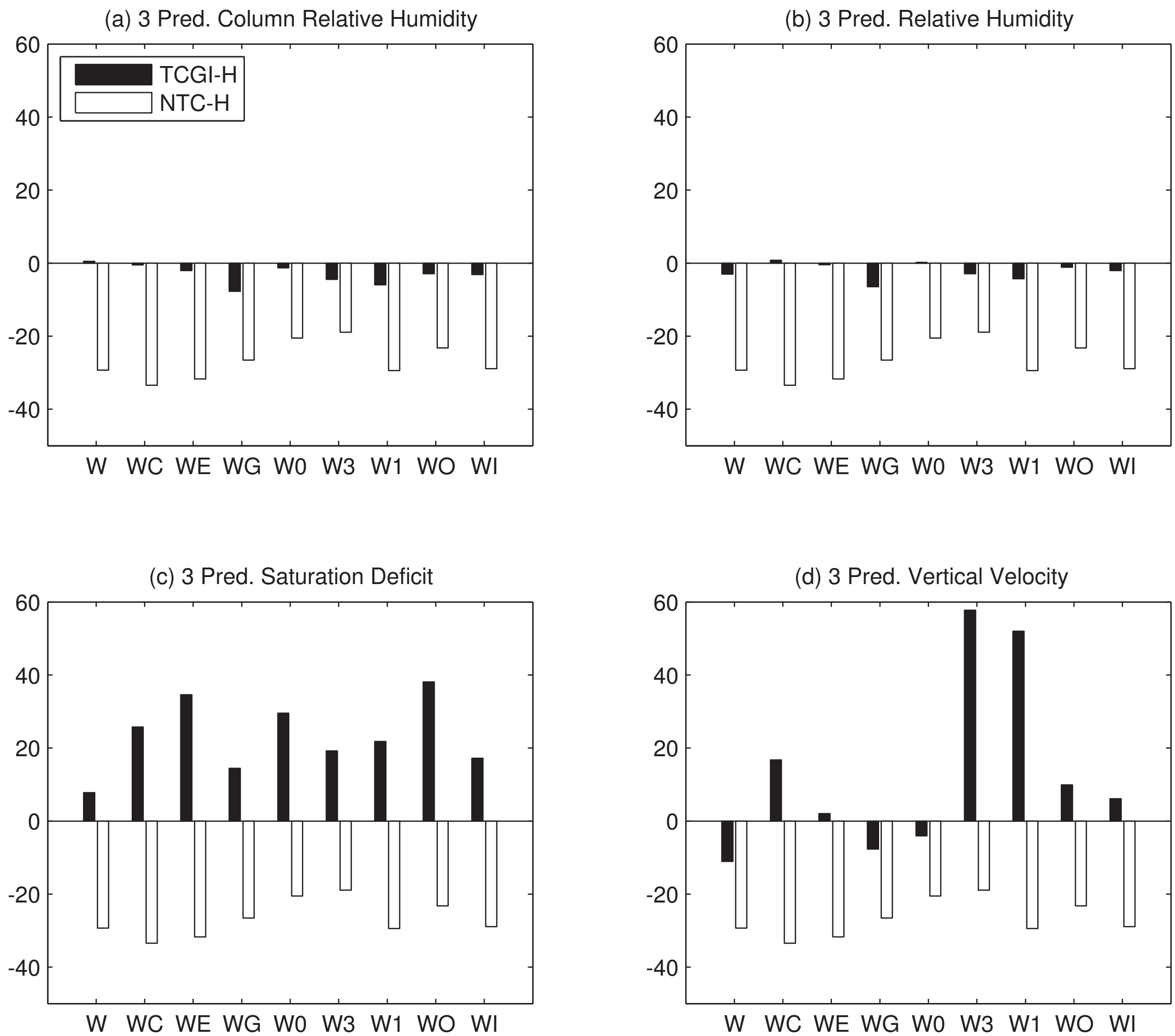

FIG. 15. Difference of globally integrated indices (black bars) in the future (all warm scenarios) and the control simulation, using as predictors low-level vorticity, vertical wind shear, and either (a) column relative humidity, (b) 600hPa relative humidtiy, (c) saturation deficity, (d) vertical velocity. Labels of scenarios as in Fig. 9.

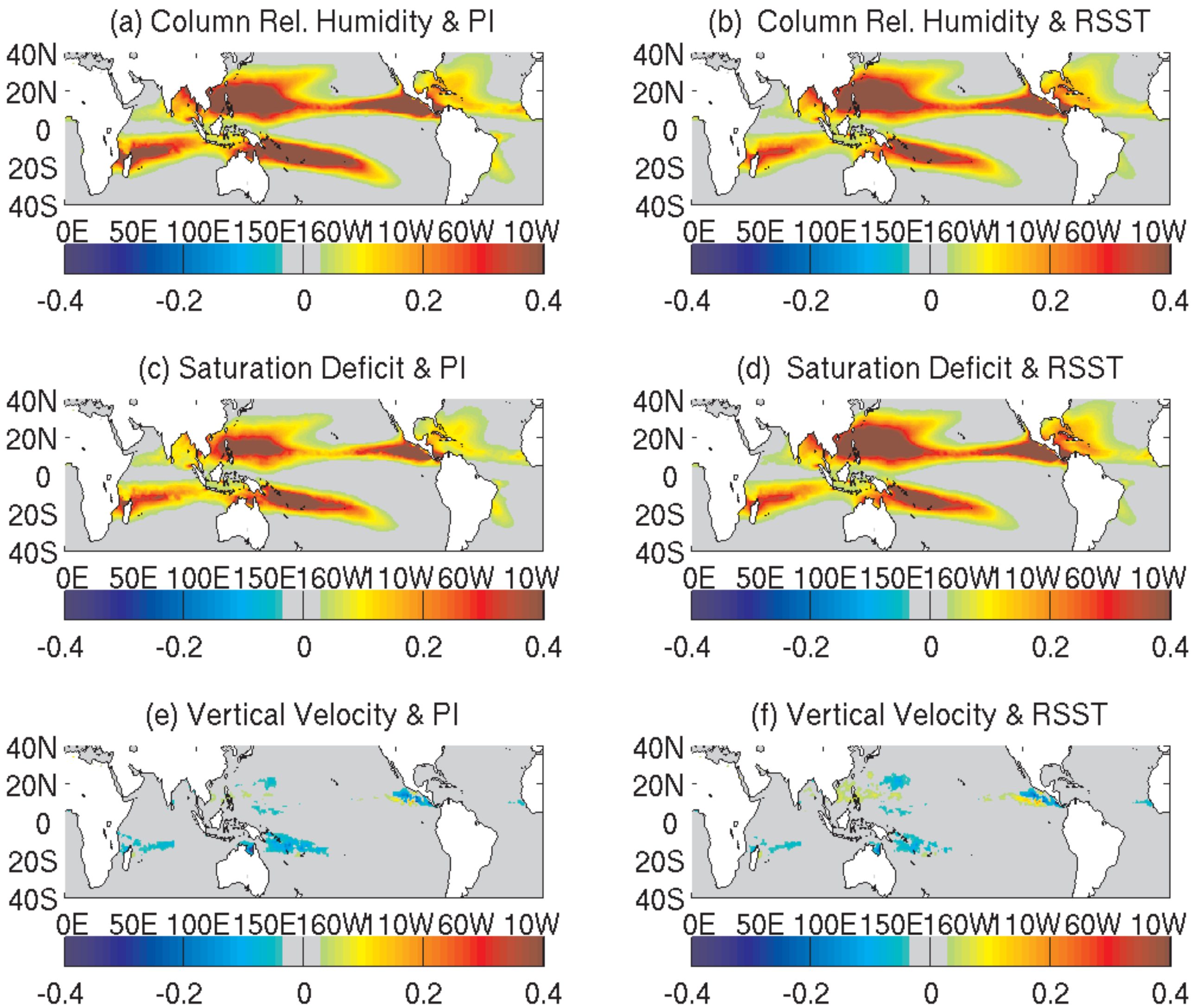

FIG. 16. Difference in the climatology of TCGI-H for the future simulations with double CO_2 and the present control simulation, using as TCGI-H predictors: vorticity, vertical shear, column relative humidity (top panels), saturation deficit (middle panels) or vertical velocity (bottom panels), as well as potential intensity (left panels) or RSST (right panels).

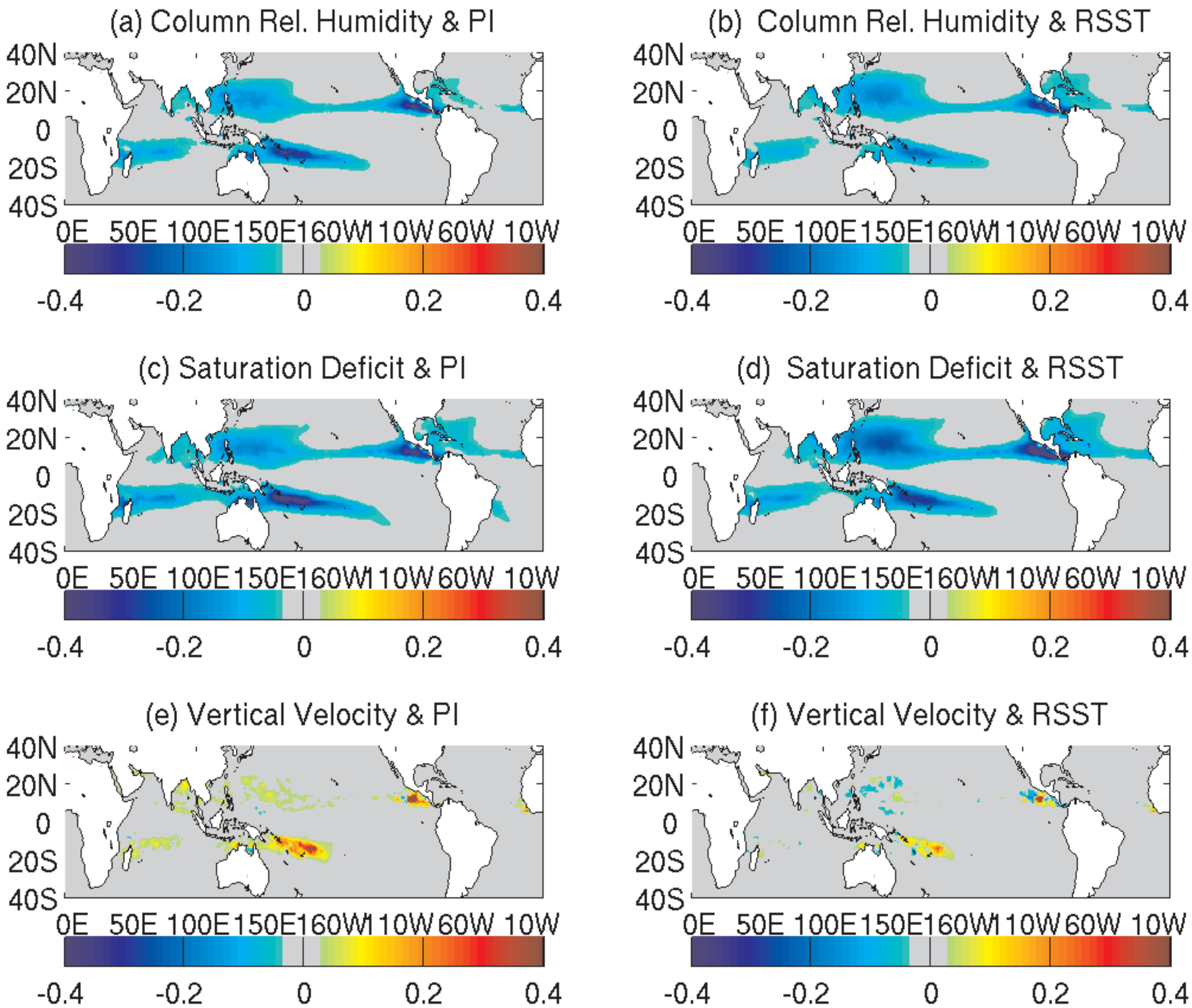

FIG. 17. Difference in the climatology of TCGI-H for the future simulations with 2K added uniformily to the SST (plus 2K) and the present control simulation, using as TCGI-H predictors: vorticity, vertical shear, column relative humidity (top panels), saturation deficit (middle panels) or vertical velocity (bottom panels), as well as potential intensity (left panels) or RSST (right panels)